transduction, *CNTFR* (ciliary neurotropic factor receptor) and *DSCR1* (Down syndrome critical region gene 1); for ECM remodeling, *MMP15* (matrix metallopeptidase 15); for ECM components, *LRRFIP1* (leucine-rich repeat interacting protein 1) and *MUC4* (mucin 4 cell surface-associated). Interestingly, we also identified two glutamate signaling-associated genes among the up-regulated genes: *HOMER1* (homer homolog 1) and *GRIN3A* (glutamate receptor ionotropic *N*-methyl-D-aspartate 3A). *HOMER1* is a glutamate receptor-binding protein, and *GRIN3A* is one of the glutamate receptor subunits. The *HOMER1* and *GRIN3A* mRNA expressions in the mechanically stressed human PDL cells were significantly up-regulated in the real-time PCR analysis (Fig. 1*B*).

Functional Expression of Glutamate Signaling-associated Molecules in Human PDL Cells—Glutamate receptors are divided into two groups: metabotropic G-protein-coupled receptors (mGluR1 to -8) and ionotropic ligand-gated channels. The ionotropic ligand-gated channels are subdivided into α-amino-3-hydroxyl-5-methyl-4-isoxazole-propionate receptors (GRIA1 to -4), kainite receptors (GRIK1 to -5), and *N*-methyl-D-aspartate receptors (NMDARs; GRIN1, GRIN2A to -2D, GRIN3A, and GRIN3B) (23). Vesicular glutamate transporters (VGLUT1 to -3) (24) and adaptor molecules, such as HOMER1, also participate in glutamate signaling (25). Through our RT-PCR analysis, we found for the first time that human PDL cells constitutively expressed the mRNAs for *mGluR2* to *-6*, *GRIA3*, *GRIN1*, *GRIN2C*, *GRIN2D*, *GRIN3B*, and *VGLUT1* (Fig. 2*A*). Similar results were observed in human PDL cells derived from three different donors (data not shown). Next, we assessed whether the glutamate receptors were functional in human PDL cells. Determination of the intracellular Ca^{2+} influx showed that 100 μM exogenous glutamate apparently increased the fluorescence intensity compared with the control cells (Fig. 2*B*). These findings showed that exogenous glutamate induced an intracellular Ca^{2+} influx, followed by glutamate signaling in human PDL cells. We also analyzed the phosphorylation of CREB, which is mediated via mGluRs (26–28) and promotes the cytodifferentiation of osteoblasts *in vitro* and *in vivo* (29). Western blotting analysis showed that glutamate stimulation induced the phosphorylation of CREB in human PDL cells (Fig. 2*C*). These results indicated that the glutamate receptors expressed on human PDL cells were functional and that intracellular glutamate signal transduction was activated.

Effects of Mechanical Stress on Glutamate Signaling in Human PDL Cells—After the application of mechanical stress to human PDL cells for 24 h, we extracted total RNA and performed RT-PCR analyses. The analyses revealed that the mechanical stress up-regulated the gene expressions of *mGluR2–6*, *VGLUT1*, *GRIN1*, *GRIN2C*, and *GRIN3B* (Fig. 3*A*). Interestingly, we also found that human PDL cells spontaneously released glutamate and that the mechanical stress significantly increased the glutamate release after 48 h (Fig. 3*B*). We then assessed whether the mechanical stress induced the phosphorylation of CREB in human PDL cells. Western blotting analyses revealed that the mechanical stress induced the phosphorylation of CREB after 48 h (Fig. 3*C*).

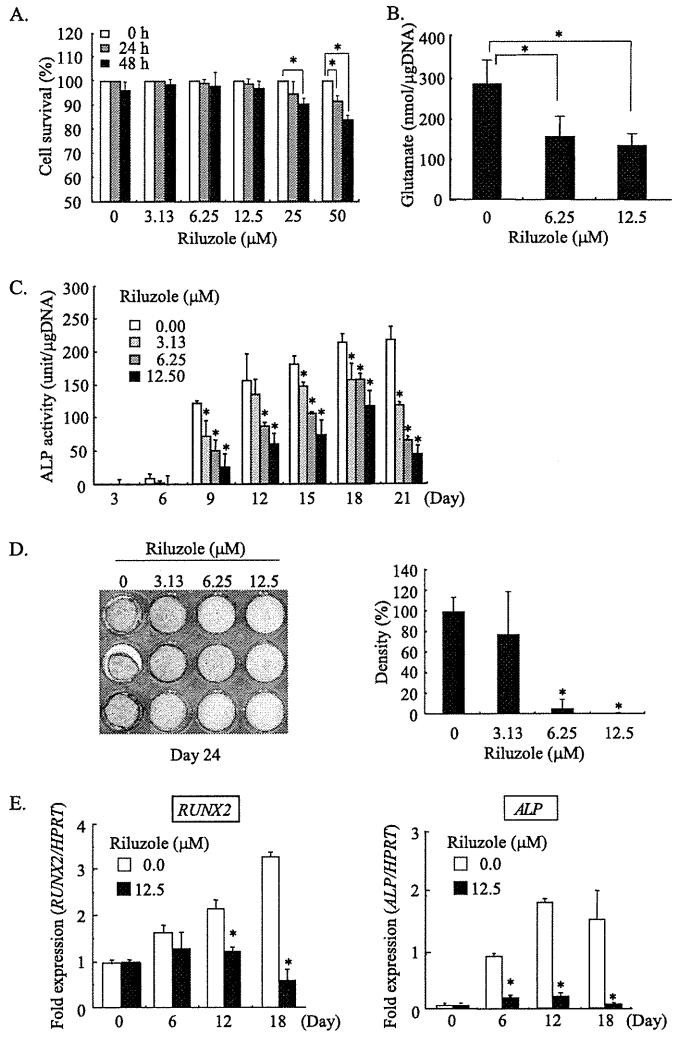

FIGURE 5. **Effects of inhibition of glutamate release on the cytodifferentiation and mineralization of human PDL cells.** *A*, the viabilities of human PDL cells were assessed after incubation in the presence or absence of riluzole for 0, 24, and 48 h. Values are shown as percentages relative to the numbers of surviving cells at 0 h. Values represent the means ± S.D. (*error bars*) of triplicate assays. Similar results were obtained in three separate experiments, and representative data are shown. *, $p < 0.05$, compared with 0 h. *B*, human PDL cells were cultured in the mineralization-inducing medium in the presence or absence of riluzole for 24 days. The release of glutamate from human PDL cells was measured on day 9. *C*, the ALP activities were analyzed. *D*, the mineralized nodule formation was analyzed on day 24. A picture of the alizarin red staining is shown on the *left*, and the densities of the alizarin red staining analyzed by the software Win ROOF are shown on the *right*. *E*, total RNA was extracted from human PDL cells during the cytodifferentiation and mineralization of the cells. Real-time RT-PCR was performed for the gene expressions of *RUNX2* and *ALP*. The *RUNX2* and *ALP* expressions were normalized by the *HPRT* expression. Values represent the means ± S.D. of triplicate assays. Similar results were obtained in three separate experiments, and representative data are shown. *, $p < 0.05$, compared with 0 μM riluzole.

Functional Analysis of Glutamate Signaling in Human PDL Cells—As shown in Fig. 4*A*, glutamate stimulation of human PDL cells up-regulated the gene expressions of *C-FOS*, *ALP*, and *RUNX2* (Runt-related transcription factor 2), which are known to be cytodifferentiation- and mineralization-related genes. These findings suggest the involvement of glutamate signaling in the cytodifferentiation and mineralization of human PDL cells. Thus, we measured the release of glutamate during the cytodifferentiation of human PDL cells into mineralized tissue-forming cells. We confirmed that the ALP activities

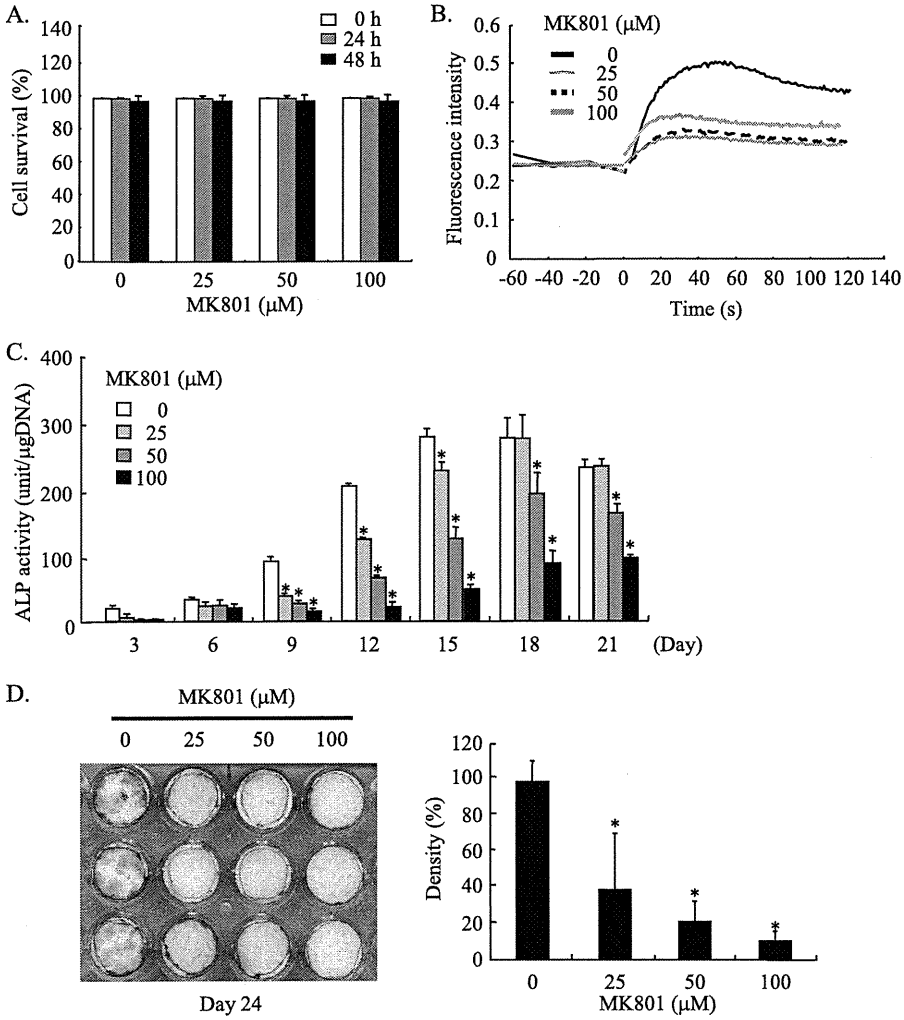

FIGURE 6. **Effects of inhibition of glutamate signaling via NMDARs on the cytodifferentiation and mineralization of human PDL cells.** *A*, the viabilities of human PDL cells were assessed after incubation in the presence or absence of MK801 for 0, 24, and 48 h. Values are shown as percentages relative to the numbers of the surviving cells at 0 h. Values represent the means ± S.D. (*error bars*) of triplicate assays. Similar results were obtained in three separate experiments, and representative data are shown. *B*, the Ca^{2+} influxes in human PDL cells in the presence or absence of MK801 were determined after stimulation of human PDL cells with 100 μM exogenous glutamate. The fluorescence intensity was measured to assess the Ca^{2+} influx into human PDL cells. Zero seconds indicates the time of the stimulation with glutamate. A representative experiment of four independent experiments is shown. *C*, human PDL cells were cultured in the mineralization-inducing medium in the presence or absence of MK801, and the ALP activities were measured. *D*, the mineralized nodule formation was analyzed on day 24. A picture of the alizarin red staining is shown on the *left*, and the densities of the alizarin red staining analyzed by the software Win ROOF are shown on the *right*. Values represent the means ± S.D. of triplicate assays. Similar results were obtained in three separate experiments, and representative data are shown. *, $p < 0.05$, compared with 0 μM MK801.

gradually increased during culture of human PDL cells in the mineralization-inducing medium for 21 days (data not shown). Under these experimental conditions, the release of glutamate from human PDL cells was increased during the process of the cytodifferentiation and reached its peak on day 9 of long term culture (Fig. 4*B*). Next, we assessed the expressions of CREB and inositol 1,4,5-trisphosphate (IP_3), which is one of second messengers of glutamate signaling via mGluRs (26). Real-time PCR analyses revealed up-regulation of CREB and IP_3 during the cytodifferentiation of PDL cells with the exact same pattern of glutamate secretion (Fig. 4*C*). These results suggested that glutamate secreted by PDL cells induces CREB and IP_3 expressions during the course of the cytodifferentiation. Subsequently, we examined the effect of the exogenous addition of glutamate on the cytodifferentiation of human PDL cells. As shown in Fig. 4*D*, the ALP activities of human PDL cells were significantly enhanced by the addition of glutamate for 15 days after the induction of the cytodifferentiation of human PDL cells. *RUNX2* expression was also significantly enhanced by the addition of glutamate during the early stage of the cytodifferentiation of human PDL cells (Fig. 4*E*). These results suggest that glutamate signaling is involved in the cytodifferentiation of human PDL cells into mineralized tissue-forming cells.

Effects of Inhibition of Glutamate Release on the Cytodifferentiation and Mineralization of Human PDL Cells—To investigate the effects of endogenous glutamate signaling on the cytodifferentiation and mineralization of human PDL cells, we utilized a glutamate release inhibitor, riluzole. First, we examined the effect of riluzole on the survival of human PDL cells. The cell survival assay showed that riluzole at 12.5 μM or less did not affect the viability of human PDL cells after a 48-h incubation (Fig. 5*A*). We then confirmed the effect of riluzole on the inhibition of glutamate release from human PDL cells. As shown in Fig. 5*B*, we found that riluzole significantly decreased the glutamate release from human PDL cells during the cytodifferentiation in a dose-dependent manner.

To examine the effects of riluzole on the cytodifferentiation and mineralization of human PDL cells, we cultured human PDL cells in the mineralization-inducing medium in the presence of riluzole. Riluzole significantly decreased the ALP activities during the cytodifferentiation of human PDL cells in a dose-dependent manner (Fig. 5*C*). The results of alizarin red staining also showed that riluzole inhibited the mineralized nodule formation on day 24 during the course of the cytodifferentiation of human PDL cells in a dose-dependent manner (Fig. 5*D*). In addition, real-time RT-PCR analysis revealed that riluzole significantly down-regulated the gene expressions of *RUNX2* and *ALP* during the cytodifferentiation of human PDL cells (Fig. 5*E*).

Effects of Inhibition of Glutamate Signaling via NMDARs on the Cytodifferentiation and Mineralization of Human PDL Cells—NMDARs are specific glutamate ionotropic receptors and are composed of heteromeric assemblies between the

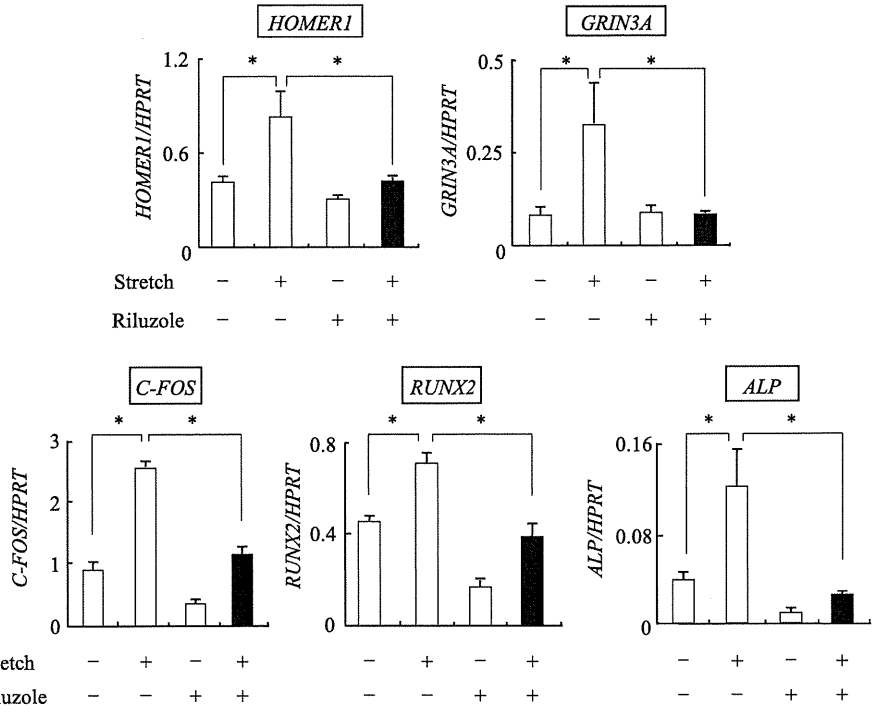

FIGURE 7. **Effects of glutamate signaling on mechanical stress-induced gene expressions.** Real-time RT-PCR was performed for the gene expressions of *HOMER1*, *GRIN3A*, *C-FOS*, *RUNX2*, and *ALP* in human PDL cells after the application of mechanical stress for 48 h in the presence or absence of riluzole (12.5 μM). Each gene expression was normalized by the *HPRT* expression. Values represent the means ± S.D. (*error bars*) of triplicate assays. Similar results were obtained in three separate experiments, and representative data are shown. *, $p < 0.05$.

essential GRIN1 subunit and the other subunits (30, 31). These receptors play an important role in the initiation of neuroplasty and modulate intracellular Ca^{2+} influx, activate Ca^{2+}-dependent enzymes such as Ca^{2+}/calmodulin-dependent protein kinases (CaMKII) and calcineurin, and regulate the phosphorylation of proteins and gene transcription (32).

To analyze the effects of glutamate signaling via NMDARs on the cytodifferentiation and mineralization of human PDL cells, we utilized an antagonist of NMDARs, MK801. First, we examined the effect of MK801 on the survival of human PDL cells. The cell survival assay revealed that MK801 at 100 μM or less had no effect on the viability of human PDL cells after a 48-h incubation (Fig. 6*A*). Human PDL cells were stimulated with 100 μM exogenous glutamate in the presence of MK801 to confirm the antagonistic effect of MK801 on the activation of NMDARs in human PDL cells. Determination of the Ca^{2+} influx showed that MK801 inhibited the fluorescence intensity in a dose-dependent manner (Fig. 6*B*).

To examine the effects of MK801 on the cytodifferentiation and mineralization of human PDL cells, we cultured human PDL cells in the mineralization-inducing medium in the presence of MK801. As shown in Fig. 6*C*, MK801 significantly suppressed the ALP activities in a dose-dependent manner during the cytodifferentiation of human PDL cells. Alizarin red staining revealed that MK801 significantly reduced the mineralized nodule formation on day 24 during the course of the cytodifferentiation and mineralization of human PDL cells (Fig. 6*D*).

Effects of Glutamate Signaling on Mechanical Stress-induced Gene Expression—To analyze the relationships among glutamate signaling, mechanical stress, and the cytodifferentiation and mineralization of human PDL cells, we examined the effects of riluzole on the cytodifferentiation and mineralization-related gene expressions in human PDL cells under mechanical stress. Real-time RT-PCR analyses demonstrated that the gene expressions of *HOMER1* and *GRIN3A* were up-regulated after a 48-h mechanical stress in the absence of riluzole. On the other hand, riluzole significantly inhibited the up-regulation of the *HOMER1* and *GRIN3A* expressions (Fig. 7, *upper panels*). Likewise, the mechanical stress-induced gene expressions of *C-FOS*, *RUNX2*, and *ALP* as cytodifferentiation and mineralization-related genes were also down-regulated in the presence of riluzole (Fig. 7, *bottom*).

In Vivo Induction of the Gene Expressions of Glutamate Signaling-associated Molecules in PDL Tissue by Orthodontic Tooth Movement—To establish the biological relevance of the *in vitro* studies to the *in vivo* situation, we investigated the gene expressions of the glutamate signaling-associated molecules in PDL tissue by utilizing a mouse model of orthodontic tooth movement (21). We selected probes for *Homer1*, *Vglut1*, *Grin1*, *mGluR3*, *mGluR5*, and *mGluR6*. The upper molar teeth were moved by an orthodontic force mediated by a closed-coil spring for 0, 12, and 24 h. We observed horizontal cross-sections of the tooth roots at the indicated time points by hematoxylin-eosin (H&E) staining (Fig. 8*A*, *a–c*). At 12 and 24 h after the application, the root was moving to the right side in each image. In Fig. 8, tension sites were created on the left side of the root, and pressure sites were present on the right side. At the indicated time points, the teeth were moving in the direction of the force within the dental sockets, and resorption and remodeling of the alveolar bone were initially activated (Fig. 8*A*, *a–c*). *In situ* hybridization analyses revealed that the PDL faintly expressed the glutamate signaling-associated molecule genes *Homer1*, *Vglut1*, *Grin1*, *mGluR3*, *mGluR5*, and *mGluR6* at the base line (Fig. 8*A*, *d*, *g*, *j*, *m*, *p*, and *s*). Of note was the observation that these gene expressions were up-regulated at the tension sites at 12 and 24 h after the application (Fig. 8*A*, *e*, *f*, *h*, *i*, *k*, *l*, *n*, *o*, *q*, *r*, *t*, and *u*). On the contrary, the mRNA expression levels of these molecules were not changed at the pressure sites at 12 and 24 h after the application (Fig. 8*A*, *e*, *f*, *h*, *i*, *k*, *l*, *n*, *o*, *q*, *r*, *t*, and *u*). We also analyzed the expressions of the cytodifferentiation and mineralization-related genes *Runx2*, type I collagen, and osteocalcin. *In situ* hybridization analyses revealed that the mRNA expression of *Runx2* was observed even in normal PDL cells (at 0 h) and thereafter was only increased at the tension sites after the application of orthodontic force (Fig. 8*B*, *a–c*). This finding indicated that cytodifferentiation of PDL cells at the tension

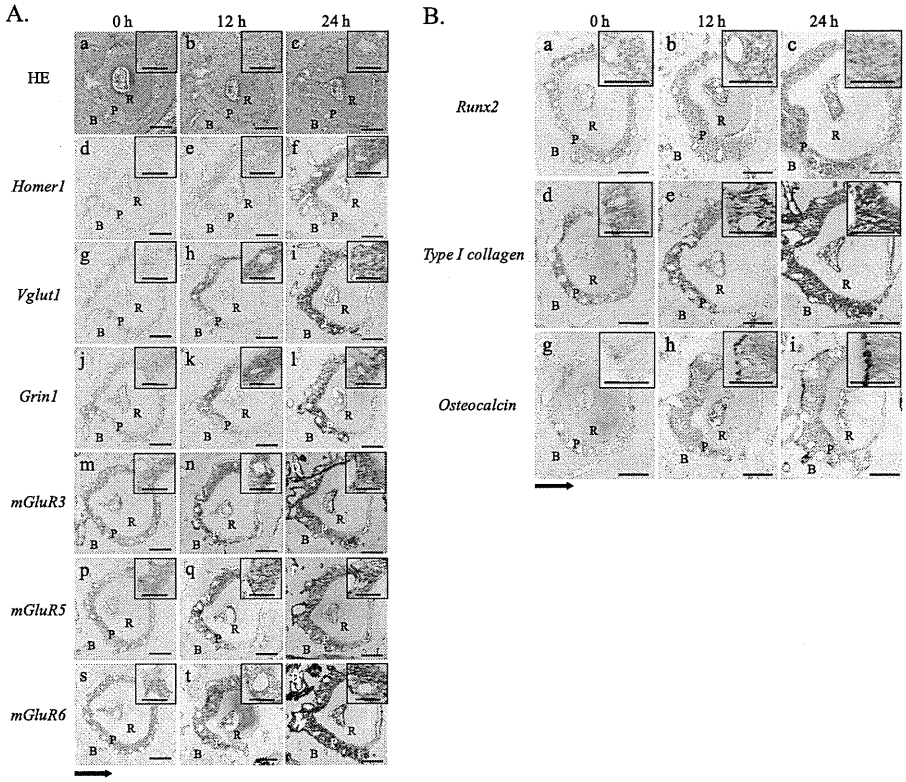

FIGURE 8. ***In vivo* induction of the gene expressions of glutamate signaling-associated molecules in PDL tissue by orthodontic tooth movement.** The upper first molars of ICR mice were moved with orthodontic force for the indicated time periods. Horizontal sections of the periodontium around the palatal root of the first molars were stained. *A*, H&E staining (*a–c*). The gene expressions of *Homer1* (*d–f*), *Vglut1* (*g–i*), *Grin1* (*j–l*), *mGluR3* (*m–o*), *mGluR5* (*p–r*), and *mGluR6* (*s–u*) were analyzed by *in situ* hybridization. *B*, the gene expressions of the cytodifferentiation and mineralization-related genes *Runx2* (*a–c*), type I collagen (*d–f*), and osteocalcin (*g–i*) were analyzed by *in situ* hybridization. *P*, PDL; *R*, root; *B*, bone. *Scale bars*, 200 μm. *Black arrow*, direction of the force application. Each *inset* shows a higher magnification image of the tension sites (*left side*). *Scale bars* in the *insets*, 100 μm.

sites was induced by the mechanical stress *in vivo*. Type I collagen was also expressed in the PDL at 0 h and then clearly up-regulated at the tension sites (Fig. 8*B*, *d–f*), indicating active synthesis of collagen fibers. Moreover, strong expression of osteocalcin was detected near the alveolar bone at the tension sites after 24 h of the force application (Fig. 8*B*, *g–i*), showing that bone remodeling was activated by mechanical tensile stress *in vivo*.

DISCUSSION

Mechanical stress is one of the most important factors for maintaining the homeostasis of a variety of tissues, such as bone, muscle, skin, and blood vessels. PDL tissues are also influenced and regulated by mechanical stresses, such as occlusal pressure and orthodontic forces. The physiological levels of the forces regulate cellular functions and remodeling of the PDL adequately, whereas pathophysiological forces can induce connective tissue destruction and bone and teeth resorption in periodontal diseases or inadequate orthodontic tooth treatments clinically.

The signaling pathways linking mechanical stress to cell functions are still not well described. In the present study, we carried out a comprehensive microarray analysis to assess the influences of physiological tensile mechanical stress on human PDL cells *in vitro* and identified the up-regulation of glutamate signaling-associated genes. We further revealed that a mechanical stretch applied to human PDL cells induced their cytodifferentiation and mineralization through activation of glutamate signaling pathways.

In this study, we identified 17 up-regulated genes, including *CNTFR*, *DSCR1*, *MMP15*, *LRRFIP1*, *PLXND1*, and *ANGPTL1*, in human PDL cells after a 48-h mechanical stress using a DNA chip analysis. Interestingly, de Araujo *et al.* (33) reported a microarray analysis of human PDL cells under compressive forces using an *in vitro* three-dimensional culture system. They identified several up-regulated genes, including inflammation-related molecules, such as *COX-2* (cyclooxygenase-2), PGE_2 (prostaglandin E_2), *IL-6* (interleukin-6), and *IL-1β* (interleukin-1β), which were not listed in our present study. These findings suggest that mechanical compressive stress tends to induce inflammation and destructive responses, whereas tensile stress induces cytodifferentiation and remodeling responses in PDL cells *in vivo*, similar to those in orthodontic treatments. *CNTFR* encodes a receptor for ciliary neurotropic factor, which is known to be a growth factor. Ciliary neurotropic factor has been implicated in the regulation of cell survival and cytodifferentiation in the brain (34). *DSCR1*, the product of a chromosome 21 gene highly expressed in the brain, is located in the minimal candidate region for the Down syndrome phenotype. DSCR1 protein encoded by the gene interacts with calcineurin A to inhibit calcineurin-dependent signaling pathways and induce anti-inflammatory reactions (35). *MMP15* is a member of the matrix metalloproteinase (MMP) family and promotes ECM remodeling (36). *LRRFIP1* (leucine-rich repeat (in FLII)-interacting protein 1), which is an ECM component, occupies a tumor necrosis factor-α (TNF-α) promoter site and appears to act as a repressor of TNF-α production (37). *PLXND1* (Plexin D1) (38) and *ANGPTL1* (angiopoietin-like 1) (39) are both associated with vasculogenesis and angiogenesis. In summary, the differentiation, proliferation, ECM remodeling, and angiogenesis induced by mechanical stress may contribute to arranging the optimal microcircumstances for the homeostasis and remodeling of PDL tissue. Among these up-regulated genes, we found two glutamate signaling-associated genes, *HOMER1* and *GRIN3A*. *HOMER1* encodes a member of the homer family of dendritic proteins and regulates intracellular Ca^{2+}. HOMER connects group 1 mGluRs, such as mGluR1 and mGluR5, to other scaffolding proteins (40). *GRIN3A* encodes a subunit of NMDAR, which

belongs to the superfamily of glutamate-regulated ion channels. Further analyses revealed that in addition to *HOMER1* and *GRIN3A*, human PDL cells constitutively and functionally expressed glutamate signaling-associated molecules, including glutamate and its receptors. We also demonstrated that the application of mechanical stress to human PDL cells up-regulated the expressions of glutamate signaling-associated genes, increased the secretion of glutamate from the cells, and induced intracellular signal transduction. These results reveal that mechanical stress activates glutamate signaling pathways in human PDL cells.

Recently, glutamate signaling has been reported to be involved in bone metabolism (41). There are some similarities between PDL cells and osteoblasts, in that PDL cells can differentiate into mineralized tissue-forming cells when they are cultured in mineralization-inducing medium *in vitro* (42). The induction of the cytodifferentiation of human PDL cells increased the release of glutamate from human PDL cells as well as CREB and IP_3 transcription. Exogenous glutamate enhanced the ALP activities and *RUNX2* expression during the cytodifferentiation of human PDL cells. These results suggest that glutamate signaling promotes the cytodifferentiation and mineralization of human PDL cells. The suppression of ALP activities and calcified nodule formation of human PDL cells by riluzole, an inhibitor of glutamate release, and MK801, an antagonist of NMDARs, strengthens the notion that glutamate signaling is crucial for the cytodifferentiation and mineralization of human PDL cells. The analyses utilizing MK801 suggested that glutamate signaling via NMDARs contributes to the enhancement of the cytodifferentiation and mineralization of human PDL cells. The effects of antagonists for other glutamate receptors on the cytodifferentiation and mineralization of human PDL cells warrant further investigation.

Mechanical stress has been reported to induce the expressions of cytodifferentiation and mineralization-related genes in osteoblasts (43). However, the molecular mechanism of the activation of osteoblasts that leads to bone remodeling has not been fully elucidated. In this study, we confirmed that human PDL cells up-regulated the gene expressions of *C-FOS*, *RUNX2*, and *ALP* under mechanical stress. On the other hand, riluzole inhibited the up-regulation of the mechanical stress-induced gene expressions of *C-FOS*, *RUNX2*, and *ALP*. These results suggest that glutamate signaling controls the upstream of the mechanical stress-induced gene expressions and clearly demonstrate the involvement of glutamate signaling in the mechanical stress-induced cytodifferentiation and mineralization of human PDL cells.

Orthodontic tooth movement has been defined as the result of biological responses to mechanical stress applied to a tooth and is achieved by PDL and alveolar bone remodeling. Bone formation and resorption are induced at the tension sites and pressure sites, respectively. The *in situ* hybridization analyses revealed that the expressions of the glutamate signaling-associated genes *Homer1*, *Vglut1*, *Grin1*, *mGluR3*, *mGluR5*, and *mGluR6* were clearly up-regulated in the tension sites of the PDL under orthodontic tooth movement *in vivo*. Up-regulation of the cytodifferentiation and mineralization-related genes *Runx2*, type I collagen, and osteocalcin was observed in the tension sites. These findings strongly support our *in vitro* data indicating that glutamate signaling was induced by the tensile mechanical stress and promoted the cytodifferentiation and mineralization of PDL cells. According to a previous report that tensile force activates PDL cells and modulates PDL remodeling by the induction of ECM synthesis and degradation (32), we consider that the glutamate signaling-associated molecules are also modulated together with the activation of PDL cells and PDL remodeling in response to mechanical stress.

In conclusion, we have demonstrated that mechanical stress induces glutamate signaling in the PDL, resulting in enhancement of the cytodifferentiation and mineralization of PDL cells. These findings suggest that mechanical stress-induced glutamate signaling is involved in the homeostasis, remodeling, and regeneration of periodontal tissue.

Acknowledgments—We thank Dr. Kaori Izutsu and Dr. Tetsuya Iida (Laboratory of Genomic Research on Pathogenic Bacteria, International Research Center for Infectious Diseases, Research Institute for Microbial Diseases, Osaka University, Japan) for technical support for the scanning and analysis of the DNA chips.

REFERENCES

1. Wang, J. H., and Thampatty, B. P. (2006) *Biomech. Model Mechanobiol.* **5,** 1–16
2. Henneman, S., Bildt, M. M., Degroot, J., Kuijpers-Jagtman, A. M., and Von den Hoff, J. W. (2008) *Arch. Oral Biol.* **53,** 161–167
3. Ozaki, S., Kaneko, S., Podyma-Inoue, K. A., Yanagishita, M., and Soma, K. (2005) *J. Periodontal Res.* **40,** 110–117
4. Takano-Yamamoto, T., Takemura, T., Kitamura, Y., and Nomura, S. (1994) *J. Histochem. Cytochem.* **42,** 885–896
5. Domon, S., Shimokawa, H., Yamaguchi, S., and Soma, K. (2001) *Eur. J. Orthod.* **23,** 339–348
6. Pavlin, D., and Gluhak-Heinrich, J. (2001) *Crit. Rev. Oral Biol. Med.* **12,** 414–424
7. Vignery, A., and Baron, R. (1980) *Anat. Rec.* **196,** 191–200
8. Cohn, S. A. (1965) *Arch. Oral Biol.* **10,** 909–919
9. Kaneko, S., Ohashi, K., Soma, K., and Yanagishita, M. (2001) *J. Periodontal Res.* **36,** 9–17
10. Hollmann, M., O'Shea-Greenfield, A., Rogers, S. W., and Heinemann, S. (1989) *Nature* **342,** 643–648
11. Torii, K., and Cagan, R. H. (1980) *Biochim. Biophys. Acta.* **627,** 313–323
12. Bertrand, G., Gross, R., Puech, R., Loubatières-Mariani, M. M., and Bockaert, J. (1992) *Br. J. Pharmacol.* **106,** 354–359
13. Patton, A. J., Genever, P. G., Birch, M. A., Suva, L. J., and Skerry, T. M. (1998) *Bone* **22,** 645–649
14. Skerry, T. M., and Genever, P. G. (2001) *Trends Pharmacol. Sci.* **22,** 174–181
15. Somerman, M. J., Archer, S. Y., Imm, G. R., and Foster, R. A. (1988) *J. Dent. Res.* **67,** 66–70
16. Matsuda, N., Yokoyama, K., Takeshita, S., and Watanabe, M. (1998) *Arch. Oral Biol.* **43,** 987–997
17. Nicholls, D. G., and Sihra, T. S. (1986) *Nature* **321,** 772–773
18. Bessay, O. A., Lowry, O. H., and Brock, M. J. (1946) *J. Biol. Chem.* **164,** 321–329
19. Labarca, C., and Paigen, K. (1980) *Anal. Biochem.* **102,** 344–352
20. Dahl, L. K. (1952) *Proc. Soc. Exp. Biol. Med.* **80,** 474–479
21. Sakai, Y., Balam, T. A., Kuroda, S., Tamamura, N., Fukunaga, T., Takigawa, M., and Takano-Yamamoto, T. (2009) *J. Dent. Res.* **88,** 345–350
22. Yamaguchi, N., Chiba, M., and Mitani, H. (2002) *Arch. Oral Biol.* **47,** 465–471
23. Wisden, W., and Seeburg, P. H. (1993) *Curr. Opin. Neurobiol.* **3,** 291–298
24. Moriyama, Y., and Yamamoto, A. (2004) *J. Biochem.* **135,** 155–163

25. Ango, F., Robbe, D., Tu, J. C., Xiao, B., Worley, P. F., Pin, J. P., Bockaert, J., and Fagni, L. (2002) *Mol. Cell. Neurosci.* **20,** 323–329
26. Niswender, C. M., and Conn, P. J. (2010) *Annu. Rev. Pharmacol. Toxicol.* **50,** 295–322
27. Mao, L., and Wang, J. Q. (2003) *J. Neurochem.* **84,** 233–243
28. Harris, S. L., Cho, K., Bashir, Z. I., and Molnar, E. (2004) *Mol. Cell. Neurosci.* **25,** 275–287
29. Siddappa, R., Martens, A., Doorn, J., Leusink, A., Olivo, C., Licht, R., van Rijn, L., Gaspar, C., Fodde, R., Janssen, F., van Blitterswijk, C., and de Boer, J. (2008) *Proc. Natl. Acad. Sci. U.S.A.* **105,** 7281–7286
30. Iemata, M., Takarada, T., Hinoi, E., Taniura, H., and Yoneda, Y. (2007) *J. Cell. Physiol.* **213,** 721–729
31. Monyer, H., Sprengel, R., Schoepfer, R., Herb, A., Higuchi, M., Lomeli, H., Burnashev, N., Sakmann, B., and Seeburg, P. H. (1992) *Science* **256,** 1217–1221
32. Malenka, R. C., and Nicoll, R. A. (1999) *Science* **285,** 1870–1874
33. de Araujo, R. M., Oba, Y., and Moriyama, K. (2007) *J. Periodontal Res.* **42,** 15–22
34. Müller, S., Chakrapani, B. P., Schwegler, H., Hofmann, H. D., and Kirsch, M. (2009) *Stem Cells* **27,** 431–441
35. Fuentes, J. J., Genescà, L., Kingsbury, T. J., Cunningham, K. W., Pérez-Riba, M., Estivill, X., and de la Luna, S. (2000) *Hum. Mol. Genet.* **9,** 1681–1690
36. English, J. L., Kassiri, Z., Koskivirta, I., Atkinson, S. J., Di Grappa, M., Soloway, P. D., Nagase, H., Vuorio, E., Murphy, G., and Khokha, R. (2006) *J. Biol. Chem.* **281,** 10337–10346
37. Suriano, A. R., Sanford, A. N., Kim, N., Oh, M., Kennedy, S., Henderson, M. J., Dietzmann, K., and Sullivan, K. E. (2005) *Mol. Cell. Biol.* **25,** 9073–9081
38. Kanda, T., Yoshida, Y., Izu, Y., Nifuji, A., Ezura, Y., Nakashima, K., and Noda, M. (2007) *J. Cell. Biochem.* **101,** 1329–1337
39. Lai, D. M., Li, H., Lee, C. C., Tzeng, Y. S., Hsieh, Y. H., Hsu, W. M., Hsieh, F. J., Cheng, J. T., and Tu, Y. K. (2008) *Neurochem. Int.* **52,** 470–477
40. Roche, K. W., Tu, J. C., Petralia, R. S., Xiao, B., Wenthold, R. J., and Worley, P. F. (1999) *J. Biol. Chem.* **274,** 25953–25957
41. Chenu, C., Serre, C. M., Raynal, C., Burt-Pichat, B., and Delmas, P. D. (1998) *Bone* **22,** 295–299
42. Piche, J. E., Carnes, D. L., Jr., and Graves, D. T. (1989) *J. Dent. Res.* **68,** 761–767
43. Nomura, S., and Takano-Yamamoto, T. (2000) *Matrix Biol.* **19,** 91–96

Journal of Cellular Physiology

Fibroblast Growth Factor-2 Stimulates Directed Migration of Periodontal Ligament Cells via PI3K/AKT Signaling and CD44/ Hyaluronan Interaction

YOSHIO SHIMABUKURO, HIROAKI TERASHIMA, MASAHIDE TAKEDACHI, KENICHIRO MAEDA, TOMOMI NAKAMURA, KEIGO SAWADA, MARIKO KOBASHI, TOSHIHITO AWATA, HIROYUKI OOHARA, TAKANOBU KAWAHARA, TOMOAKI IWAYAMA, TOMOKO HASHIKAWA, MANABU YANAGITA, SATORU YAMADA, AND SHINYA MURAKAMI*

Division of Oral Biology and Disease Control, Department of Periodontology, Osaka University Graduate School of Dentistry, Osaka, Japan

Fibroblast growth factor-2 (FGF-2) regulates a variety of functions of the periodontal ligament (PDL) cell, which is a key player during tissue regeneration following periodontal tissue breakdown by periodontal disease. In this study, we investigated the effects of FGF-2 on the cell migration and related signaling pathways of MPDL22, a mouse PDL cell clone. FGF-2 activated the migration of MPDL22 cells and phosphorylation of phosphatidylinositol 3-kinase (PI3K) and akt. The PI3K inhibitors, Wortmannin and LY294002, suppressed both cell migration and akt activation in MPDL22, suggesting that the PI3K/akt pathway is involved in FGF-2-stimulated migration of MPDL22 cells. Moreover, in response to FGF-2, MPDL22 showed increased CD44 expression, avidity to hyaluronan (HA) partly via CD44, HA production and mRNA expression of HA synthase (Has)-1, 2, and 3. However, the distribution of HA molecular mass produced by MPDL22 was not altered by FGF-2 stimulation. Treatment of transwell membrane with HA facilitated the migration of MPDL22 cells and an anti-CD44 neutralizing antibody inhibited it. Interestingly, the expression of CD44 was colocalized with HA on the migrating cells when stimulated with FGF-2. Furthermore, an anti-CD44 antibody and small interfering RNA for CD44 significantly decreased the FGF-2-induced migration of MPDL22 cells. Taken together, PI3K/akt and CD44/HA signaling pathways are responsible for FGF-2-mediated cell motility of PDL cells, suggesting that FGF-2 accelerates periodontal regeneration by regulating the cellular functions including migration, proliferation and modulation of extracellular matrix production.

J. Cell. Physiol. 226: 809–821, 2011.

Cell migration is essential for embryogenesis, tissue development, wound healing, and tissue regeneration. This cellular event requires coordinated multiple processes such as activation of related signaling pathways, membrane-linked cytoskeleton reorganization, causing specific structural changes in the plasma membrane, and interaction with the extracellular matrix.

Phosphatidylinositol 3-kinase (PI3K) is associated with cell polarization and migration in a wide range of cell types (Derman et al., 1997; Ren and Schwartz, 1998; Cantley, 2002; Weiner et al., 2002). Polarized accumulation of phospholipid PI(3,4,5)P3 and its product is seen via PI3K for establishment of cell polarity and migration during chemotaxis. In addition, PI3K and its downstream kinase effector akt are known to regulate cytoskeletal rearrangements, cell migration, apoptosis, and other biological functions.

As one of the key extracellular matrices involved in cell migration, hyaluronan (HA) has been receiving particular attention. HA is a linear glycosaminoglycan composed of repeating disaccharides of glucuronic acid and *N*-acetylglucosamine: [β1,4-GlcUA- β1,3-GlcNAc-] and is ubiquitously distributed in the body. HA is synthesized at the inner face of the plasma membrane by HA synthase (Has). A wide variety of mediators regulate the HA synthesis and in turn modulate physiological and pathophysiological conditions via HA. So far, HA has been reported to be involved in not only matrix organization, but also cell adherence, cell migration, cell proliferation. In the early phase of tissue repair, enhanced expression of HA precedes other glycosaminoglycan (Lamm et al., 2001), leading to facilitation of cell motility and subsequent tissue remodeling.

CD44, a cell surface molecule, is one of the major receptors for HA. The intracellular portion is linked to actin filaments and mediates intracellular signal transduction. Interestingly, CD44 has been reported to be present on the leading edge of migrating cells (Thorne et al., 2004). The interaction of CD44 with HA activates Rac1 and in turn regulates the formation of cytoskeleton-mediated membrane protrusions and cell migration (Bourguignon et al., 2000). Myoblasts derived from CD44-deficient mouse lacked the chemotaxis seen in the wild-type myoblasts (Mylona et al., 2006). In addition, CD44-deficient fibroblasts revealed less directional migration and less efficiency of wound closure in wound healing assay in spite of the increased motility compared with the wild type (Acharya

Contract grant sponsor: Research Fellow of the Japan Society for the Promotion of Science;
Contract grant numbers: 20390529, 20390530, 20592427, 21592623, 21659482, 21890137, 22592182.

*Correspondence to: Shinya Murakami, 1-8 Yamadaoka, Suita, Osaka 565-0871, Japan. E-mail: ipshinya@dent.osaka-u.ac.jp

Received 15 October 2009; Accepted 17 August 2010

Published online in Wiley Online Library (wileyonlinelibrary.com), 20 September 2010.
DOI: 10.1002/jcp.22406

et al., 2008). Upon injury of the central nervous system, CD44 expression was increased at the site of injury (Jones et al., 2000). In addition, CD44/HA interaction plays an important role in regulating astrocyte functions such as cell migration following injury (Bourguignon et al., 2007). These results suggest that CD44 regulates several coordinated actions required for physiologically efficient motility, which contributes to the integrated wound healing.

Periodontal disease is initiated by bacterial biofilm and exacerbated with multi-factors, resulting in the loss of tooth-supporting periodontal tissues such as gingiva, alveolar bone, periodontal ligament (PDL), and cementum covering root surface. Unfortunately, no conventional periodontal treatment, such as scaling and root planning, can ever regenerate periodontal tissue destroyed by progression of periodontal diseases. Interestingly, however, several lines of evidence have demonstrated that topical application of recombinant cytokine to the destroyed site can induce regeneration of the periodontal tissues. We have shown that fibroblast growth factor-2 (FGF-2) induces significant periodontal tissue regeneration accompanying new alveolar bone and cementum formation in beagle dogs and macca monkey (Murakami et al., 1999, 2003; Takayama et al., 2001). Recently, a randomized controlled Phase II clinical trial revealed significant increase in the rate of increase in alveolar bone height in the 0.3% FGF-2 treatment group (Kitamura et al., 2008, 2010). In vitro studies have revealed that FGF-2 induces potent proliferative responses and regulates the expression of a variety of extracellular matrices by PDL cells, which play critical roles in wound healing and regeneration of periodontal tissue (Takayama et al., 1997; Shimabukuro et al., 2005; Terashima et al., 2008; Murakami, 2010). Notwithstanding the importance of migratory action of PDL cells during the process of periodontal tissue regeneration, the effects of FGF-2 on its migratory activity remain uncertain. Here we use MPDL22, a mouse PDL clone, to explore the mechanism by which FGF-2-induced migration of PDL cells. The present study revealed that FGF-2 upregulated the migration of PDL cells and that its activity is dependent on PI3K/akt and the CD44/HA signaling pathway.

Materials and Methods

Materials

Tissue culture supplies and plastic Leighton tubes were obtained from Corning Coster (New York, NY). Alpha modification of Eagle's medium (α-MEM) was a product of ICN Biomedicals, Inc. (Costa Mesa, CA). Fetal calf serum (FCS) was purchased from JRH Biosciences (Lenexa, KS). Human recombinant FGF-2 was kindly provided by Kaken Pharmaceutical Co., Ltd (Tokyo, Japan). Wortmannin, LY294002, akt inhibitor II, and akt inhibitor X were obtained from Sigma (St. Louis, MO), Cell Signaling (Danvers, MA), and Calbiochem (Darmstadt, Germany), respectively. Anti-CD44 antibody (clone IM7) and FITC-labeled rat anti-mouse CD44 antibody (clone IM7) were obtained from BD Pharmingen (Franklin Lakes, NJ).

Isolation of mouse periodontal cell clones

Mouse PDL cells were isolated from healthy PDL tissue of first premolar teeth of BALB/c mice. The PDL tissues isolated from the center of the root surface with a surgical scalpel were minced, transferred to plastic Leighton tubes and cultured in α-MEM supplemented with 10% FCS, 50 units/ml penicillin G and 50 μg/ml streptomycin (henceforth denoted standard medium) with media changes every 2 or 3 days. Cultures were maintained at 37°C in a humidified atmosphere of 95% air and 5% CO_2. The cells that grew out from the explants and in a confluent stage were separated by treatment with 0.05% trypsin–0.53 mM EDTA, collected by centrifugation, and cultured on plastic culture dishes containing the standard medium until they reached confluence. The cells (parent PDL cells) were then trypsinized at a 1:3 split ratio. We established 29 clones from parent PDL cell lines by culturing with FGF-2 (1 μg/ml) and dilution twice. We selected one of these clones: one clone, MPDL22, differentiated cells in the presence of a high level of alkaline phosphatase (ALPase) and formed hard tissue in the presence of β-glycerophosphate and ascorbic acid (Yamada et al., 2007).

Chemotaxis and cell migration assay

In this study two migration assays (membrane filter assay and silicon restraint migration assays) were utilized to determine the implication of FGF-2 on MPDL22 motility and the mechanism underlying its effects.

Chemotaxis assay

Cell migration assays were performed by using a Chemicon QCM™ 96-well migration assay kit (Chemicon Int., Inc., Temecula, CA), according to the instruction manual. A cell suspension (5×10^4 cells/well) was added to the upper chamber of an insert membrane filter with a pore size of 8 μm. In some experiments, the insert membrane was coated with 50 μl of 1% HA (from rooster comb: MW 600,000–1,200,000) (Seikagaku Co., Tokyo, Japan) or chondroitin sulfate C (CS) (chondroitin 6-sulfate) (from shark cartilage) (Seikagaku Co.). The medium containing 1% FCS supplemented with or without FGF-2 was placed in the lower chamber of the insert membrane. At the end of incubation at 37°C in a humidified 95% air/5% CO_2 atmosphere, cells migrated to the bottom of the insert membrane were dissociated from the membrane when incubated with cell detachment buffer. These cells were subsequently lysed and detected by the CyQuant GR dye (Invitrogen Corp, Carlsbad, CA). The intensity of fluorescence was measured with a fluorescence plate reader (Thermo Electron Oy., Vantaa, Finland) using 485/538 nm filter set.

Cell migration assay

Another migration assay was conducted with a modified Teflon restraint migration assay (Smith et al., 2004). MPDL22 were seeded behind a silicon rubber on a coverglass (Matsunami Co., Osaka, Japan) mounted on a 35-mm dish and allowed to reach confluence. After carefully removing the silicon rubber, the monolayers of MPDL22 were incubated with or without FGF-2 (5 ng/ml) for 12 h. Photographs were taken using a microscope (Nikon, Tokyo, Japan). The number of cells migrating into the cell-free space was counted using NIS-Elements (Nikon) at least in five areas per coverglass.

PI3K and akt assay

PI3K and akt expression were assayed by using Face® PI3K p85 and akt kit (Active Motif, Carlsbad, CA) according to the manufacturer's instructions, respectively. Cells (1×10^5 cells/well) were seeded in a 96-well plate and cultured with or without FGF-2 (5 ng/ml). At the end of incubation, the cells were fixed with 100 μl of 4% formaldehyde in PBS for 20 min at room temperature. The cells were washed three times with washing buffer (0.1% Triton X-100 in PBS), added quenching buffer (washing buffer containing 1% H_2O_2 and 0.1% azide) and incubated for 20 min at room temperature. After incubation with antibody blocking buffer and washing with washing buffer, 40 μl of primary antibody was added to the wells, which were then incubated overnight at 4°C. After the plates were washed, 100 μl of horseradish peroxidase-conjugated anti-rabbit IgG antibody was added to the wells, followed by incubation for 1 h. After the plates were washed, 100 μl of developing solution was added and the plates were incubated for 2–20 min at room temperature until the reaction was stopped with stop solution. Absorbance was then measured using a microplate reader Model 680 (BioRad Laboratories, Inc., Hercules, CA) at 450 nm.

Cell proliferation assay (WST-1 assay)

MPDL22 cells (2×10^4 cells/well) were cultured for 24 h in a serum-free medium to obtain quiescent cells. The quiescent cells were cultured with or without FGF-2 (5 ng/ml) in the presence of 1% FCS and then treated with 10% proliferation reagent WST-1 (Roche Diagnostics GmbH, Mannheim, Germany) for the last 2 h. Absorbance (OD 450 nm) was measured using a microplate reader Model 680 (BioRad Laboratories, Inc.). In some experiments, MPDL22 was treated with or without mitomycin C (2.5 μg/ml) (Kyowa Hakko Kirin Co., Tokyo, Japan) for 2 h before FGF-2 stimulation.

Measurement of HA in culture supernatants

MPDL22 cells were placed in a 6-well culture plate (Corning Coster) at 2×10^5 cells/well in a standard medium. Forty-eight hours after incubation, MPDL22 cells were stimulated with or without FGF-2 (5 ng/ml) in the presence of 0.5% FCS. At the end of the incubation periods, the supernatants were collected and stored at −20°C until determination of HA. The HA levels in culture supernatants were measured by an inhibition binding-protein assay (HA assay kit, Seikagaku Co.), which utilizes the inhibitory reaction of free HA in samples to the binding of biotinylated HA-binding protein to HA–bovine serum albumin (BSA) (Sigma), a neo-glycoconjugate prepared from HA and BSA (Raja et al., 1984).

Agarose electrophoresis

HA samples were electrophoresed on a 0.75% agarose gel for 6 h at room temperature with a constant voltage of 25 V as described in a previous report (Lee and Cowman, 1994). Known molecular mass HA standards (300, 8,000, 2,200 kDa) were used as a reference. After electrophoresis, the HA in the gel was blotted onto Hybond N+ membrane (Amersham biosciences Corp., Piscataway, NJ). After blocking with 10% skim milk in PBS containing 0.05% Tween 20 the membrane was incubated with biotynylated HABP (1 μg/10 ml) (Seikagaku Co.) in PBS with Blockace (Snow Brand Milk Products Co. Ltd, Tokyo, Japan) at room temperature for 1 h and then with HRP–streptavidin (0.5 μg/10 ml) (Calbiochem, Inc., San Diego, CA). HA was visualized by enhanced chemiluminescence assay (GE Healthcare UK Ltd, Buckinghamshire, England).

Western blot analysis

MPDL22 cells were placed on a 6-well culture dish and stimulated with FGF-2 (5 ng/ml). Cells were lysed in RIPA buffer (25 mM Tris–HCl pH 7.6, 150 mM NaCl, 1% NP-40, 1% sodium deoxycholate, 0.1% SDS, 10 mM Na_3VO_4, 10 μg/ml each aprotinin and leupeptin). Proteins were separated by SDS/PAGE, transferred to nitrocellulose membranes. Membranes were incubated with 10% bovine serum albumin for 1 h and subsequently with mouse monoclonal anti-phosphorylated akt antibody (Cell Signaling), rabbit polyclonal antibody to phosphorylated p85 (Cell Signaling) or rat anti-mouse CD44 antibody (BD) for 3 h at room temperature and appropriate HRP-conjugated secondary antibody. Immune complex was detected using an enhanced chemiluminescence kit (GE Healthcare UK Ltd).

Flow cytometric analysis

MPDL22 cells were incubated in 10% FCS–α-MEM in the absence or presence of FGF-2 (5 ng/ml). The cells were harvested with cell dissociation buffer (Sigma) and incubated with rat anti-mouse CD44 antibody (BD) on ice for 30 min. After washed twice with 1% BSA supplemented with 0.1% sodium azide, cells were incubated FITC-labeled-goat polyclonal anti-rat IgG (Invitrogen Corp) or FITC-labeled sodium HA (PG Research, Tokyo, Japan). Flow cytometric analysis was then performed with a FACS Calibur (BD).

Immunocytochemical analysis

MPDL22 cells (5×10^4 cells/well) were cultured on a glass bottom dish (Matsunami Co.) mounted on a 35-mm plate. The confluent monolayers were cultured for 24 h with or without 5 ng/ml of FGF-2.

Phalloidin and HA binding protein staining

Cells were fixed for 10 min in 4% paraformaldehyde and treated with or without 0.1% Triton X to permeabilize cell membrane. After blocking with 1% BSA in PBS, the cell monolayers were incubated with FITC-phalloidin (Invitrogen Corp), or biotinylated HA binding protein (Seikagaku Co.) in PBS for 30 min at room temperature, and then washed with 1% BSA in PBS three times between each step. Cells were then incubated with avidin–FITC (BD) for 30 min.

Actin staining

Cells were fixed with cold ethanol for 15 min. Following incubation with 3% BSA in PBS at room temperature for 30 min, the cells were incubated with mouse anti-F and G actin antibody (Abcam plc, Cambridge, UK) in PBS containing 0.1% BSA and 5% FCS for 30 min. After washing with PBS, the cells were incubated with Alexa Fluor 488-conjugated goat anti-mouse IgG (Invitrogen Corp) at room temperature for 30 min.

CD44 staining

Cells were fixed for 10 min in 4% paraformaldehyde and treated with or without 0.1% Triton X to permeabilize cell membrane. After blocking with 1% BSA in PBS, the cells were incubated with rat anti-mouse CD44 (BD) followed by washing with PBS. Then, they were incubated with Alexa Fluor 546-conjugated goat anti-rat antibody (Invitrogen Corp). In some experiments, after the fixation and permeabilization, the cells were incubated FITC-labeled rat anti-mouse CD44 antibody. All cells were counterstained with 4,6-diamidino-2-phenylindole dihydrochloride (DAPI) (Sigma) to facilitate estimates of total cell numbers, and washed once in water. All photographs were taken using a confocal laser scanning microscope (Carl Zeiss, Inc., Oberkochen, Germany), and quantified using LSM510-V2.5 (Carl Zeiss, Inc.).

Real-time PCR

MPDL22 cells were seeded at a density of 1×10^6 cells/dish in a 60 mm dish and grown to confluence in standard medium. Following a 24-h incubation of the cells with or without FGF-2 (5 ng/ml), total RNA was isolated from each cell by RNAzol™ (Cinna/Biotecx Laboratories, Inc., Friendswood, TX) according to the manufacturer's instructions. The precipitated RNA was resolved in 0.1% diethylpyrocarbonate-treated distilled water (DEPC-treated H_2O). cDNA synthesis and amplification via PCR were performed according to the methods described by Takayama et al. (1997). For PCR analysis, we incubated a 40 μl cDNA synthesis reaction mixture per RNA sample at 37°C for 60 min. Each 40 μl cDNA synthesis reaction mixture contained: 5.2 μl of DEPC-treated H_2O; 4 μl 10× PCR buffer II (100 mM Tris–HCl pH 8.3, 500 mM KCl (Perkin Elmer Cetus, Norwalk, CT)); 6 μl 25 mM $MgCl_2$; 4 μl of each 10 mM deoxynucleotide–triphosphate (Takara, Shiga, Japan); 0.4 μl 20 U/ml RNase inhibitor (Perkin Elmer Cetus); 1 μl 50 U/ml M-MLV reverse transcriptase; 4 μl 0.25 mg/ml RNA sample. After incubation, all samples were heated to 94°C for 5 min to inactivate the reverse transcriptase. Real-time PCR with SYBR Green PCR Master Mix (Applied Biosystems, Foster City, CA) was carried out by 7300 Fast real-time PCR system (Applied Biosystems) using the following primers: Has-1 (forward primer, 5′-TACCTGCGCCAGTGCTTGAC-3′: reverse primer, 5′-CACCATGAGCACGCGTAACC-3′). Has-2 (forward primer, 5′-GTCATGTACACAGCCTTCAGAGCAC-3′: reverse primer, 5′-GGCAGGGTCAAGCATAGTAATCTGAG-3′).

Has-3 (forward primer, 5′-GTCATGTACACAGCCTTCAGA-GCAC-3′: reverse primer, 5′-TACATTGCACACAGCCAAAG-TAGGA-3′), Hyal-1 (forward primer, 5′-CCGTAATGCCCTA-CGTCCAGA-3′: reverse primer, 5′-AAGGGCCCAAGTGT-GGAATC-3′), Hyal-2 (forward primer, 5′-GCTCAGCTGGCG-TCATCTTC-3′: reverse primer, 5′-GCACTGGGTCCAACTGC-AATAC-3′), Hyal-3 (forward primer, 5′-CTCGGCATTGTAG-CCAACCAC-3′: reverse primer, 5′-TGGGCTGTACCTCTA-GGTCCAAAG-3′), Hyal-4 (forward primer, 5′-TGTCTACAC-ACAGCTGGGCTACAA-3′: reverse primer, 5′-AATCAGAA-TTCACAAAGCGGTTCAC-3′), Hyal-5 (forward primer, 5′-CTATAATGAAAGTGCAGGTGGTGAG-3′: reverse primer, 5′-ATTTGGTGCAACAGGTGAGAA-3′), Spam-1 (Ph-20) (forward primer, 5′-CTTGAAGTCCAATCGACAAGCTACC-3′: reverse primer, 5′-GTACCCAGAGCAACAATTTCACCA-3′), and reduced glyceraldehyde 3-phosphate dehydrogenase (GAPDH) (forward primer, 5′-TGTGTCCGTCGTGGATCTGA-3′: reverse primer, 5′-TTGCTGTTGAAGTCGCAGGAG-3′). GAPDH served as a housekeeping gene.

Fourth PCR cycles were performed, and the cycle threshold values were normalized to the housekeeping GAPDH.

RNA silencing

Small interfering RNA (siRNA) for mouse CD44 was designed according to the sequence of the mouse CD44 gene [NCBI accession number AJ251594 (GenBank)] obtained from the online database of the National Center for Biotechnology Information (NCBI, Bethesda, MD). A sequence, 5-GGCUUUCAACAGU-ACCUUATT-3 (sense strand complementary to the exon 13 of the mouse CD44 gene), was chosen and verified in a basic local alignment search tool search of the database. The CD44 siRNA and a negative control siRNA (Silencer® negative control #1 siRNA) were synthesized by Applied Biosystems. Silencer® Negative control #1 siRNA was designed to have no significant sequence similarity to mouse, rat, or human transcript sequences. MPDL22 cells were placed on a 6-well culture dish at 7.5×10^4 cells/well in standard medium without antibiotics. Twenty-four hours after

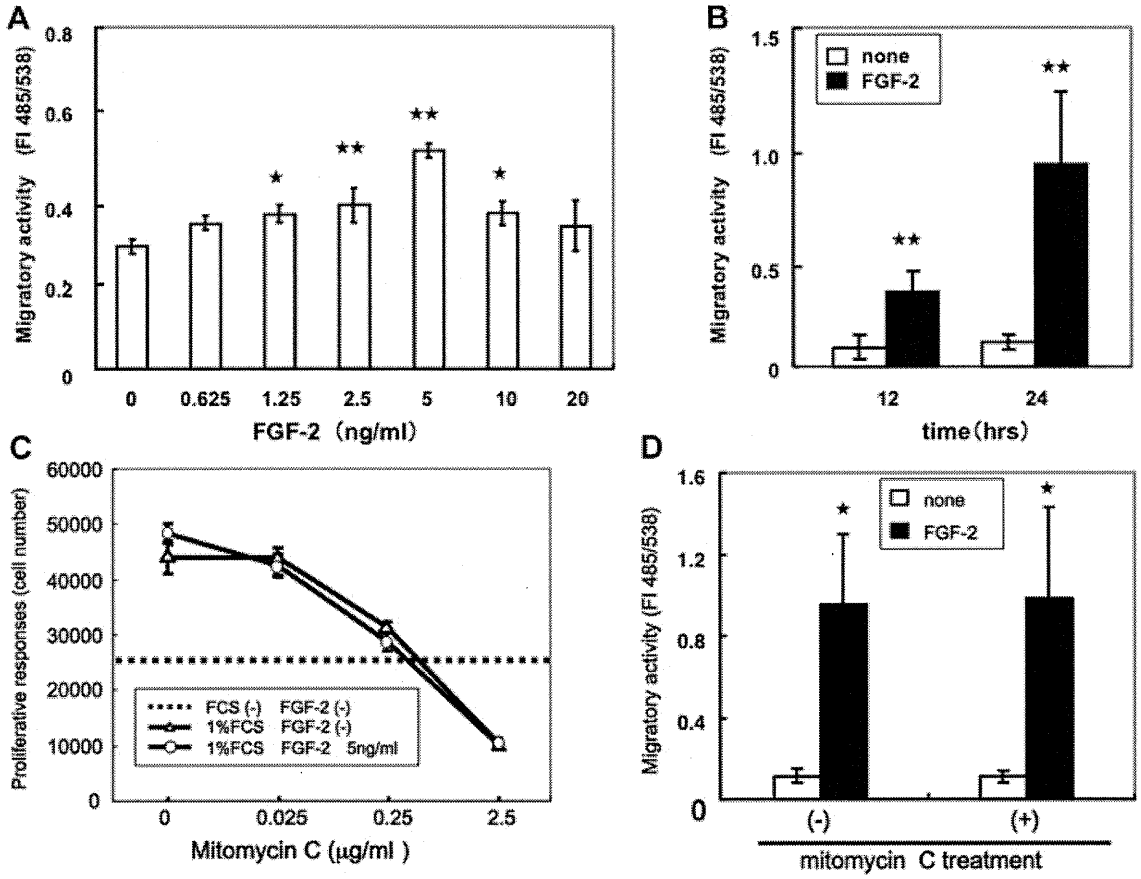

Fig. 1. FGF-2 stimulates cell motility of MPDL22 in a dose-dependent manner. A: MPDL22 cells (5×10^4 cell/well) were added to the upper chamber of an insert membrane filter of 8 μm pore size in 96-well culture plates and stimulated with or without FGF-2 (0–20 ng/ml) for 12 h. Migratory cells on the bottom of the insert membrane were dissociated from the membrane with cell detachment buffer. These cells were subsequently lysed and detected by the CyQuant GR dye. The intensity of fluorescence was measured with a fluorescence plate reader (*$P < 0.05$ vs. corresponding unstimulated control, **$P < 0.01$ vs. corresponding unstimulated control). B: MPDL22 cells were stimulated with or without FGF-2 (5 ng/ml) for 12 or 24 h. The migratory activities were assessed as described above ($P < 0.01$ vs. correspondent unstimulated control). C: MPDL22 which had been treated with or without mitomycin C for 2 h were added to a 96-well plate and were incubated with or without FGF-2 (5 ng/ml) in the presence or absence of 1% FCS for 12 h. Proliferative responses were estimated by using proliferative reagent WST-1. The dotted line shows the proliferative response of MPDL22 when the cell cultured without FCS and FGF-2. D: MPDL22 cells (5×10^4 cell/well) which had been treated with or without 2.5 μg/ml mitomycin C for 2 h were added to the upper chamber of an insert membrane filter with a pore size of 8 μm in 96-well culture plates and stimulated with or without FGF-2 (5 ng/ml) for 24 h. Migratory cells on the bottom of the insert membrane were dissociated from the membrane with cell detachment buffer. These cells were subsequently lysed and detected by the CyQuant GR dye. The intensity of fluorescence was measured with a fluorescence plate reader (*$P < 0.01$ vs. correspondent unstimulated control). Results of one representative experiment out of three separate experiments are shown. The results are presented as mean value ± SEM (n = 3).**

incubation, MPDL22 at 40–50% confluence were transfected with siRNA CD44 and negative control siRNA. The cells were transfected with 200 pmol of siRNA and negative control siRNA using lipofectamine 2000 (Invitrogen Corp) according to the manufacturer's instructions. The cells were then studied for real-time PCR, flow cytometry, and Western blot analysis.

Statistical analysis

Three specimens in each group were analyzed. Data were expressed as means and standard deviation for each group. Results of one representative experiment out of three separate experiments are shown since the values vary among the same experiment performed at different times. Statistical analysis was performed with *t*-test or ANOVA followed by Dunnett multiple comparison test. The level of significance was set at $P < 0.05$.

Results

FGF-2 increased the migratory activity of MPDL22 cells

A cell migration assay using a transwell membrane was performed to examine the effects of FGF-2 on the migratory activity of MPDL22. FGF-2 increased the migratory activity of MPDL22 cells in a dose-dependent manner up to 5 ng/ml at 12 h after stimulation (Fig. 1A). At less than 5 ng/ml FGF-2 should have a dominant influence on other cellular responses and the migratory effect of FGF-2 should be weak. Importantly, at 5 ng/ml, FGF-2-dependent proliferative responses were not observed at 12 h (data not shown). At 10 ng/ml, the migratory activity of MPDL22 cells decreased but remained significantly high compared with the unstimulated level. A significant increase of MPDL22 migratory activity was also observed 24 h after stimulation with 5 ng/ml FGF-2 (Fig. 1B).

To minimize any influence of the proliferative response on the migratory activity, we treated MPDL22 cells with mitomycin C. As shown in Figure 1C, we confirmed that 2.5 μg/ml of mitomycin C treatment inhibited the proliferative response of both FGF-2-stimulated and unstimulated MPDL22. Interestingly, there was significant FGF-2-dependent migratory activity of MPDL22 cells 24 h after FGF-2 stimulation even when the proliferative response of MPDL22 was suppressed by treatment with mitomycin C at 2.5 μg/ml (Fig. 1D).

PI3K and akt are involved in FGF-2-induced migration of MPDL22

FGF receptors mediate biological functions of MPDL22 and various molecules are involved in their intracellular signal transduction. PI3K and akt are known to be downstream molecules of FGF receptors and play critical roles in the motility of various cell types. We then investigated the involvement of PI3K and akt in the migratory activity of MPDL22. As shown in Figure 2A, treatment of MPDL22 with 5 ng/ml FGF-2 leads to upregulation of PI3K and akt activities. Western blot analysis also revealed that FGF-2 increased the level of both phospho-PI3K and phospho-akt (Fig. 2B).

Akt is known to be a major PI3K target in a wide range of cells. In order to confirm that akt is activated following PI3K stimulation upon FGF-2 treatment, Wortmannin and LY294002, both of which are PI3K inhibitors, were used in the akt ELISA assay. Both inhibitors completely suppressed the FGF-2-incresed akt activity (data not shown). These results indicate that akt is a key effector of the lipid kinase PI3K in MPDL22 cells in response to FGF-2. We then investigated the effects of PI3K/akt pathway on FGF-2-induced cell migration. We performed a migration assay using the same inhibitors to explore the involvement of PI3K and akt pathways in the migratory activity in FGF-2-stimulated MPDL22. The assay revealed that 2 nM Wortmannin or 2 μM LY294002 partially but significantly inhibited the FGF-2-induced migration activity

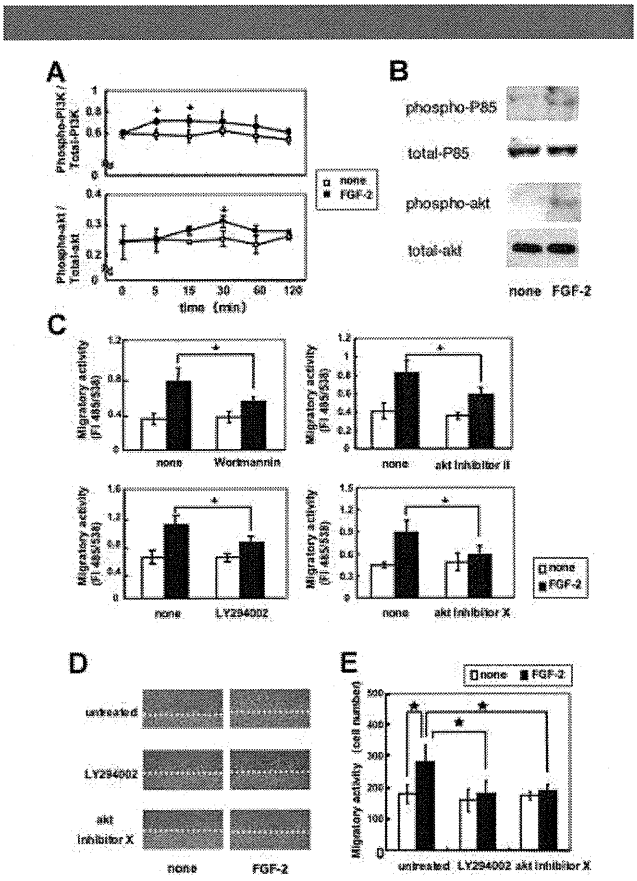

Fig. 2. FGF-2-activated cell migration is mediated by phosphorylation of PI3K and akt in MPDL 22. A: MPDL22 cells (1×10^5 cells/well) were cultured in 96-well culture plates in the presence or absence of FGF-2 (5 ng/ml). At the end of culture period, the cells were fixed with 4% paraformaldehyde for 20 min. The ratio of phospho-PI3K/total PI3K and phospho-akt/total akt was assayed by an enzyme-linked immunosorbent assay. Results of one representative experiment out of three separate experiments are shown. The results are presented as mean value ± SEM (n = 3) (*$P < 0.05$ vs. 0 min). B: MPDL22 cells (1×10^5 cells/well) were cultured in the presence or absence of FGF-2 (5 ng/ml) for 5 min. At the end of culture period, cells were lysed with RIPA buffer. Proteins were separated by SDS/PAGE, transferred to nitrocellulose membranes, and probed with anti-phospho-p85 or anti-phospho-akt antibody and HRP-conjugated secondary antibody. As a control, total p85 or akt was detected using anti-p85 or akt antibody. Results of one representative experiment out of three separate experiments are shown. C: MPDL22 cells (5×10^4 cell/well) were added to the upper chamber of an insert membrane filter with a pore size of 8 μm in 96-well culture plates and stimulated with or without FGF-2 (5 ng/ml) in the presence or absence of Wortmannin (2 nM), LY294002 (2 μM), akt inhibitor II (50 nM) or akt inhibitor X (5 nM) for 12 h. Migratory cells on the bottom of the insert membrane were dissociated from the membrane with cell detachment buffer. These cells were subsequently lysed and detected by CyQuant GR dye. The intensity of fluorescence was measured with a fluorescence plate reader. Results of one representative experiment out of three separate experiments are shown. The results are presented as mean value ± SEM (n = 3) (*$P < 0.05$). D: MPDL22 cells (5×10^4 cell/well) were seeded behind a silicon rubber on a coverglass mounted on a 35-mm dish and allowed to reach confluence. After carefully removing the silicon rubber, the monolayers were incubated with or without FGF-2 (5 ng/ml) in the presence of LY294002 (2 μM) or Akt inhibitor X (5 nM), or absence of the inhibitors. At the end of culture period, cells were fixed for 10 min in 4% paraformaldehyde. Dotted lines are the margin of the cell monolayers at the start of culture. Results of one representative experiment out of three separate experiments are shown. E: The number of cells migrating into the cell-free area were counted as described in the Materials and Methods Section. The results are presented as mean value ± SEM (n = 3) (*$P < 0.05$). [Color figure can be viewed in the online issue, which is available at wileyonlinelibrary.com.]

(Fig. 2C). On the other hand, treatment of PDL cells with 2 nM Wortmannin or 2 μM LY294002, the concentration at which FGF-2-induced cell migration was inhibited, did not significantly change cell proliferation either in the presence or absence of FGF-2 stimulation (data not shown). Furthermore, as well as PI3K inhibitor, both akt inhibitor II and X partially but significantly suppressed the enhancement of PDL cell migration induced by FGF-2 (Fig. 2C).

Moreover, in order to confirm the engagement of PI3K and akt pathways in the migratory responses of MPDL22 triggered by FGF-2, we used a restraint migration assay system in which PDL cells were cultured in a confined area behind a silicon rubber placed in the dish and the cells could migrate from the monolayers into the cell-free space after removal of the silicon rubber. As shown in Figure 2D,E, FGF-2 enhanced the cell migration into the cell-free space, which was similar to the observation obtained by the transwell assay (Fig. 1A,B). When MPDL22 cells were cultured in the presence of LY294002 and akt inhibitor X, the FGF-2-induced migration was reduced to the basal level (Fig. 2E).

FGF-2 promoted lamellipodia formation and CD44 expression in migrating cells

Upon exposure of cells to a stimulus that promotes cell migration, cells were activated with subsequent rearrangement of actin filaments, formation of cell polarization and redistribution of several adhesion molecules to leading edge. A modified silicon sheet restraint migration assay was then performed to explore the effect of FGF-2 on the formation of lamellipodia. Activation of MPDL22 with FGF-2 led to augmentation of cell migration into cell-free space with increased magnitude of lamellipodia formation (Fig. 3A,C). There was significant formation of lamellipodia on MPDL22 cells 12 h after FGF-2 stimulation. FGF-2-activated cells elongated with prominent protrusive processes. Reorganized actin at the cortex was observed in the elongated cells with prominent protrusive processes. Treatment of MPDL22 with FGF-2 resulted in a fibroblastic cell shape with increased actin stress fibers, indicating that FGF-2 influences cell morphology in MPDL22 through reorganization of the actin cytoskeleton (Fig. 3B).

CD44, a receptor for various extracellular matrices, is reported to play a crucial role in cell migration (Legg et al., 2002; Fanning et al., 2005). FACS analysis revealed that MPDL22 constitutively expressed CD44 and that 5 ng/ml of FGF-2 elevated CD44 expression by MPDL22 (Fig. 4A). The immunocytochemical study also revealed that FGF-2 intensified CD44 expression of MPDL22 (Fig. 4B). Interestingly, intense expression of CD44 was also observed in migrating cells among stimulated populations (Fig. 4C). The localization of CD44 was relatively uniform on the cell surface of the FGF-2-stimulated

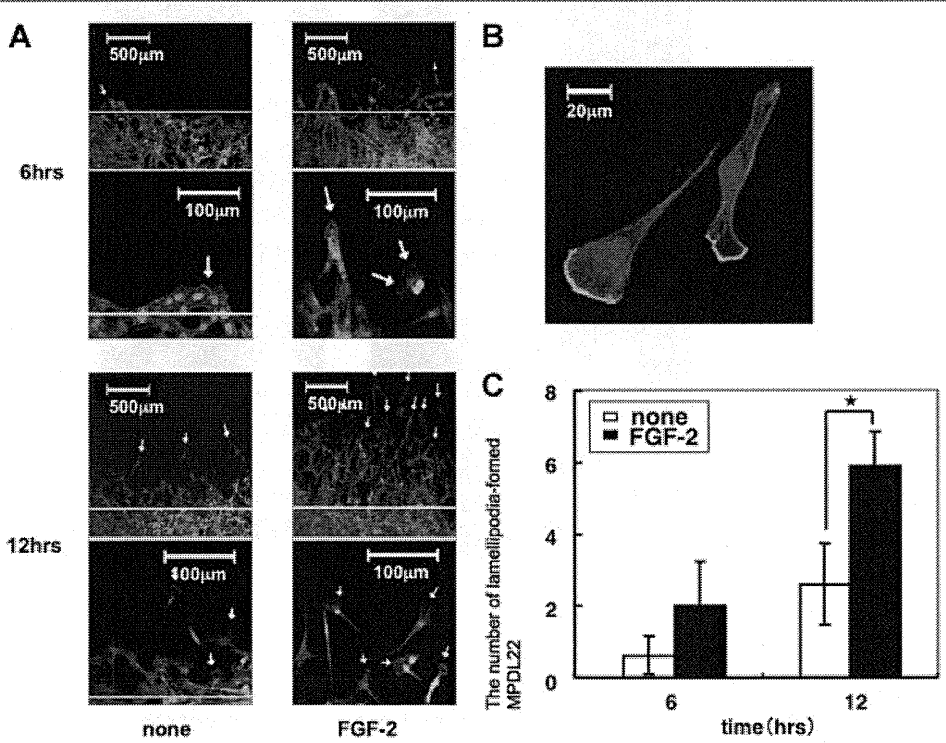

Fig. 3. FGF-2 enhanced the formation of lamellipodia in migratory MPDL22. A: MPDL22 (5×10^4 cell/well) cells were seeded behind a silicon rubber on a coverglass mounted on a 35-mm dish and allowed to reach confluence. After carefully removing the silicon rubber, the monolayers were incubated with or without FGF-2 (5 ng/ml). After incubation, cells were fixed for 10 min with 4% paraformaldehyde. After blocking with 1% BSA, the cell monolayers were incubated with FITC–phalloidin for 30 min. Dotted lines are the margin of the cell monolayers just at the culture start. Low and high power field photographs were taken at the 6th and 12th hour of culture. Results of one representative experiment out of three separate experiments are shown. B: MPDL22 cells (5×10^4 cell/well) were seeded behind a silicon rubber on a coverglass mounted on a 35-mm dish and allowed to reach confluence. After carefully removing the silicon rubber, the monolayers were incubated with FGF-2 (5 ng/ml) for 12 h. Cells were fixed with cold ethanol for 15 min. Following incubation with 3% BSA, the cells were incubated with mouse anti-F and G actin antibody in PBS containing 0.1% BSA and 5% FCS for 30 min. After washing with PBS, the cells were incubated with Alexa Fluor 488-conjugated goat anti-mouse IgG at room temperature for 30 min. C: The number of cells migrating into the cell-free area and forming lamellipodia was counted as described in the Materials and Methods Section. Results of one representative experiment out of three separate experiments are shown. The results are presented as mean value ± SEM (n = 3) ($^*P < 0.05$).

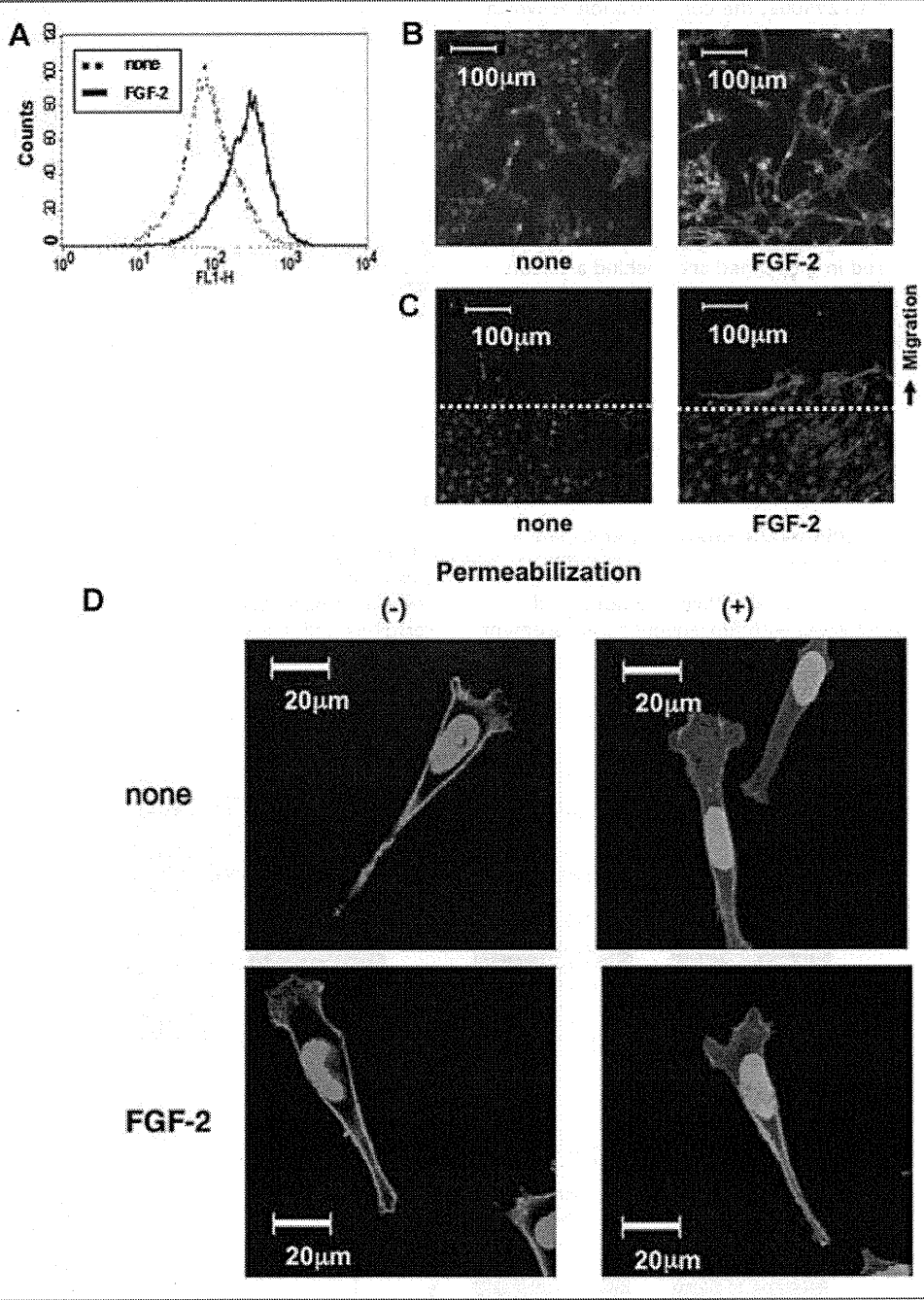

Fig. 4. FGF-2 elevated CD44 expression of MPDL22. A: MPDL22 cells (1×10^5 cell/well) were incubated in 10% FCS–α-MEM in the presence or absence of FGF-2 (5 ng/ml) for 12 h. The cells were incubated with rat anti-mouse CD44 followed by washing with PBS and FITC-labeled-goat polyclonal anti-rat IgG. Cells were analyzed by flow cytometry. Results of one representative experiment out of three separate experiments are shown. B: MPDL22 cells (5×10^4 cell/well) were cultured on a glass bottom dish mounted on a 35-mm plate. The monolayers were cultured for 24 h with or without 5 ng/ml of FGF-2. Cells were fixed for 10 min with 4% paraformaldehyde. After blocking with 1% BSA, the cell monolayers were incubated with rat anti-mouse CD44 followed by washing with PBS and Alexa Fluor 546-conjugated goat anti-rat antibody for 30 min. Cells were counterstained with DAPI. Results of one representative experiment out of three separate experiments are shown. C: MPDL22 cells (5×10^4 cell/well) were seeded behind a silicon rubber on a coverglass mounted on a 35-mm plate and allowed to reach confluence. After carefully removing the silicon rubber, the monolayers were incubated with or without FGF-2 (5 ng/ml) for 12 h. At the end of culture period, the cells were fixed for 10 min in 4% paraformaldehyde. After blocking with 1% BSA, the cell monolayers were incubated with rat anti-mouse CD44 followed by washing with PBS and Alexa Fluor 546-conjugated goat anti-rat antibody for 30 min. Cells were counterstained with DAPI. Dotted lines indicate the edge of the cell layer just after removing the silicon rubber. Results of one representative experiment out of three separate experiments are shown. D: MPDL22 cells (5×10^4 cell/well) were cultured on a glass bottom dish mounted on a 35-mm plate. The monolayers were cultured for 24 h with or without 5 ng/ml of FGF-2. Cells were fixed for 10 min in 4% paraformaldehyde and treated with or without 0.1% Triton X to permeabilize cell membrane. After blocking with 1% BSA, they were incubated with FITC-labeled rat anti-mouse CD44 antibody for 30 min. Cells were counterstained with DAPI. Results of one representative experiment out of three separate experiments are shown.

migratory cells. Although CD44 was also located in the cytoplasmic region of MPDL22, FGF-2 stimulation or migratory activity did not influence the cytoplasmic localization of CD44 in MPDL22 (Fig. 4D).

FGF-2 upregulated the expression of HA of MPDL22

By interacting with HA as a specific receptor, CD44 mediates various biological functions (Goodison et al., 1999; Pure and Cuff, 2001). Since FGF-2 increased CD44 expression on MPDL22, we speculated that CD44/HA interaction plays an important role for migration of MPDL22. As previously reported (Shimabukuro et al., 2005), FGF-2 significantly increased the HA level in the culture supernatant of MPDL22 compared to unstimulated MPDL22 (Fig. 5A). Furthermore, the immunocytochemical study also showed that exposure of MPDL22 to FGF-2 resulted in increased expression of HA while unstimulated MPDL22 revealed moderate expression of HA (Fig. 5B). We performed agarose gel electrophoresis to examine whether FGF-2 modulates the distribution of HA molecular size induced by MPDL22. The distribution of molecular size produced by FGF-2-activated MPDL22 was similar to that by unstimulated MPDL22 (Fig. 5C). HA is synthesized at the inner face of the plasma membrane by Has and degraded by hyaluronidase (Hyal). To confirm the influence of FGF-2 on HA synthesis and degradation, we

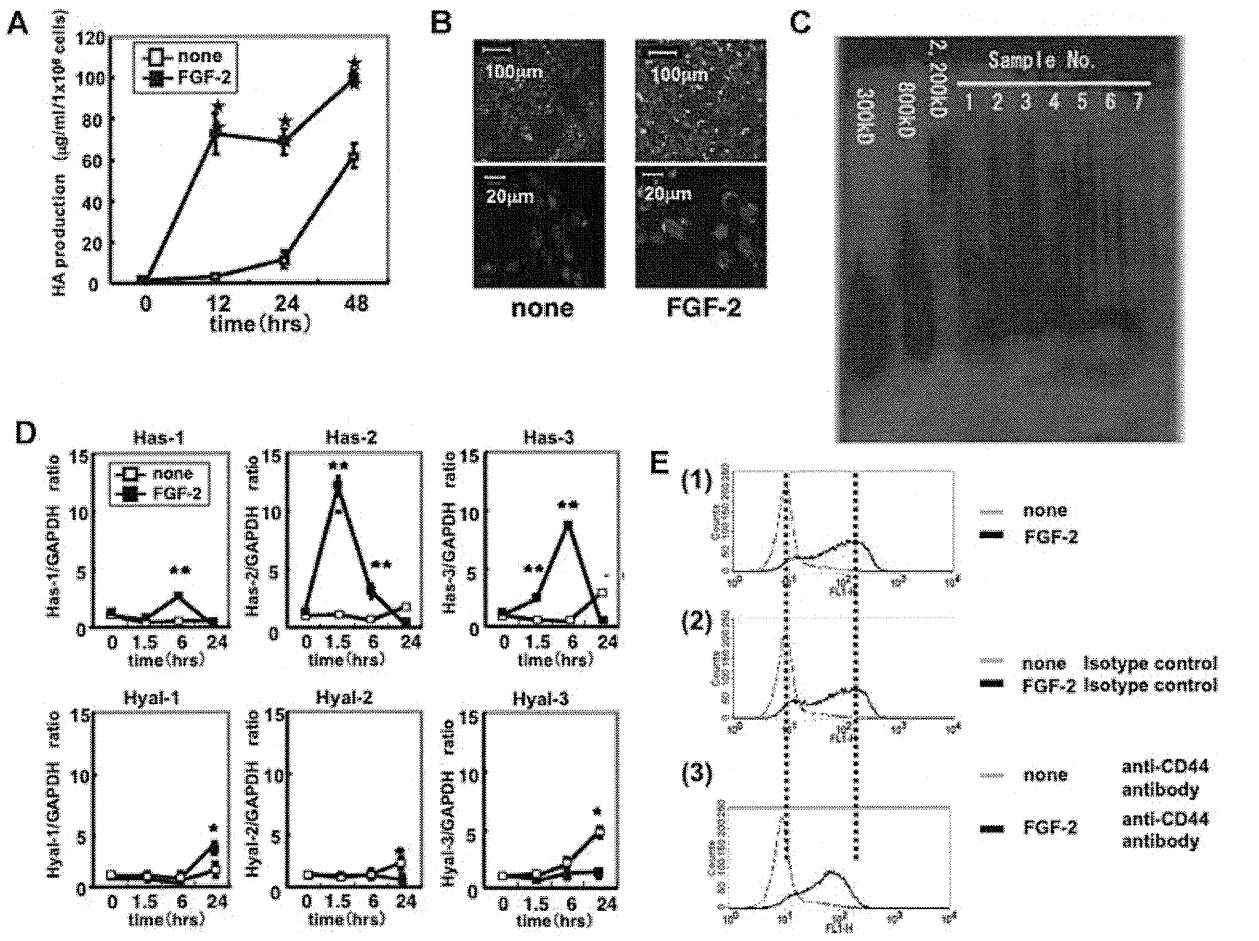

Fig. 5. Treatment of MPDL22 with FGF-2 resulted in the upregulation of HA production and binding avidity to HA via CD44. A: MPDL22 cells (2×10^5 cells/well) were cultured with or without FGF-2 (5 ng/ml) for the indicated duration and the culture supernatants were removed. The concentration of HA in the culture supernatants was assayed as described in the Materials and Methods Section. Results of one representative experiment out of three separate experiments are shown. The results are presented as mean value ± SEM (n = 3) ($^{**}P < 0.01$ vs. 0 h). B: MPDL22 cells (5×10^4 cells/well) were cultured on a glass bottom dish mounted on a 35 mm plate. Following culture in the presence or absence of FGF-2 (5 ng/ml) for 24 h, cells were fixed with 4% paraformaldehyde. Cells were treated with 1% BSA, incubated with biotinylated HA binding protein and then FITC–avidin. Cells were washed with PBS between each step. Cells were counterstained with DAPI. High power field is shown in bottom parts. Results of one representative experiment out of three separate experiments are shown. C: MPDL22 (2×10^5 cells/well) cells were incubated in 10% FCS–α-MEM in the presence or absence of FGF-2 (5 or 50 ng/ml) for 24 or 48 h. Twenty micrograms of HA in the culture medium was electrophoresed on 0.75% agarose gel. Known molecular mass HA standards (300, 800, 2,200 kDa) were used as a reference. Lane 1: none, 24 h; lane 2: none, 48 h; lane 3: 5 ng/ml of FGF-2, 24 h; lane4; 5 ng/ml of FGF-2, 48 h; lane 5: 50 ng/ml of FGF-2, 24 h; lane 6: 50 ng/ml of FGF-2, 48 h; lane 7: 10% FCS–α-MEM. D: MPDL-22 cells were seeded at a density of 1×10^5 cells/dish in a 60 mm dish and grown to confluence in standard medium. After culture for 24 h with or without FGF-2 (5 ng/ml) to activate MPDL, total RNA was isolated and cDNA synthesis was performed. Real-time PCR with SYBR Green PCR Master Mix was carried out using Has-1, Has-2, Has-3, Hyal1, Hyal2, and Hyal3 primers. GAPDH served as a housekeeping gene. PCR was performed for 40 cycles, and the cycle threshold values were normalized to the housekeeping GAPDH. Results of one representative experiment out of three separate experiments are shown. The results are presented as mean value ± SEM (n = 3) ($^{*}P < 0.05$, $^{**}P < 0.01$ vs. 0 h). E: MPDL22 cells were incubated in 10% FCS–α-MEM in the presence (black line) or absence of FGF-2 (5 ng/ml) (gray line) (1) with the isotype control antibody (2), or anti-CD44 antibody (3) for 12 h. The cells were harvested and incubated with FITC-labeled sodium HA. Cells were analyzed by flow cytometry. Results of one representative experiment out of three separate experiments are shown.

performed real-time PCR for Has gene expression of Has-1, Has-2, and Has-3 and Hyal gene expression of Hyal1, Hyal2, Hyal3, Hyal4, Hyal5, and Ph-20. FGF-2 increased Has-1, Has-2, and Has-3 mRNA expression, which was maximal from 1.5 to 6 h (Fig. 5D). In contrast, FGF-2 slightly altered Hyal1, Hyal2, and Hyal3 gene expression (Fig. 5D). Hyal4, Hyal5, and Ph-20 mRNA expression was not detected in both unstimulated and FGF-2 stimulated MPDL22 (data not shown). We then evaluated the HA-binding avidity of FGF-2-stimulated MPDL22 using FITC-labeled sodium HA. FGF-2-activated MPDL22 acquired the enhancement of adhesive avidity to HA (Fig. 5E(1)), and the FGF-2-induced HA binding to MPDL22 was inhibited by anti-CD44 neutralizing antibody (Fig. 5E(3)).

CD44-HA interaction was involved in the migration of FGF-2-stimulated MPDL22

In order to investigate the involvement of HA in MPDL22 migration, we coated the transwell membrane with HA and performed a migration assay. As shown in Figure 6A, we observed that treatment of membrane with HA resulted in a significant increase in MPDL22 migration activity while treatment with CS did not. To evaluate the involvement of CD44 in HA-dependent cell migration, we applied the anti-CD44 antibody to a migration assay system using a HA-coated membrane. The anti-CD44 antibody at 0.1 and 1 μg/ml significantly reduced FGF-2-induced cell migration to the same extent, although no inhibitory effect was observed at 0.01 μg/ml (Fig. 6B). Interestingly, the expression of CD44 in migratory cells among FGF-2-activated MPDL22 was colocalized with HA (Fig. 7A,B). We then investigated whether the CD44/HA pathway contributes to FGF-2-induced migration of MPDL22. Addition of anti-CD44 antibody to the migration assay significantly inhibited the FGF-2-dependent migration of MPDL22 (Fig. 8). Furthermore, we performed an RNA silencing experiment. As described in Figure 9A, treatment with siRNA for CD44 significantly decreased CD44 mRNA expression of MPDL22. The decrease in CD44 expression at the protein level was confirmed by flow cytometry and western blot analysis whereas the negative control siRNA had little effect (Fig. 9B,C). Interestingly, CD44 siRNA significantly inhibited the FGF-2-induced cell migration of MPDL22 in a chemotaxis assay and migration assay, although FGF-2-stimulated MPDL22 transfected with CD44 siRNA still showed significant upregulation of migratory activity compared to that of unstimulated MPDL22 transfected with the siRNA (Fig. 9D,E).

Discussion

PDL is an important tooth-supporting apparatus between the tooth and alveolar bone and is a reservoir of mesenchymal stem cells (Beertsen et al., 1997; Lekic et al., 2001; Seo et al., 2004). Rapid induction and appropriate accumulation of PDL cells are critical during the tissue healing and regeneration for successful repair and regeneration of periodontal tissues. Importantly, such cell behavior associated with the tissue repair is strictly regulated by various cytokines. FGF-2, one of those cytokines, is produced from various types of cells and is a key factor promoting wound healing and regeneration of tissues.

Cell migration is a complicated sequential action during development, physiological, and inflammatory events. The multi-step process is well coordinated and regulated by various factors, such as cytokine and growth factor, extracelluar matrix and its surface receptors on the cells. Autocrine and paracrine regulation is also observed in cell migration (Maheshwari et al., 2001). In addition, the extracellular matrix and its cell surface receptor are critical. CD44-deficient cell exhibited impaired cell migration with fewer stress fibers (Acharya et al., 2008) and

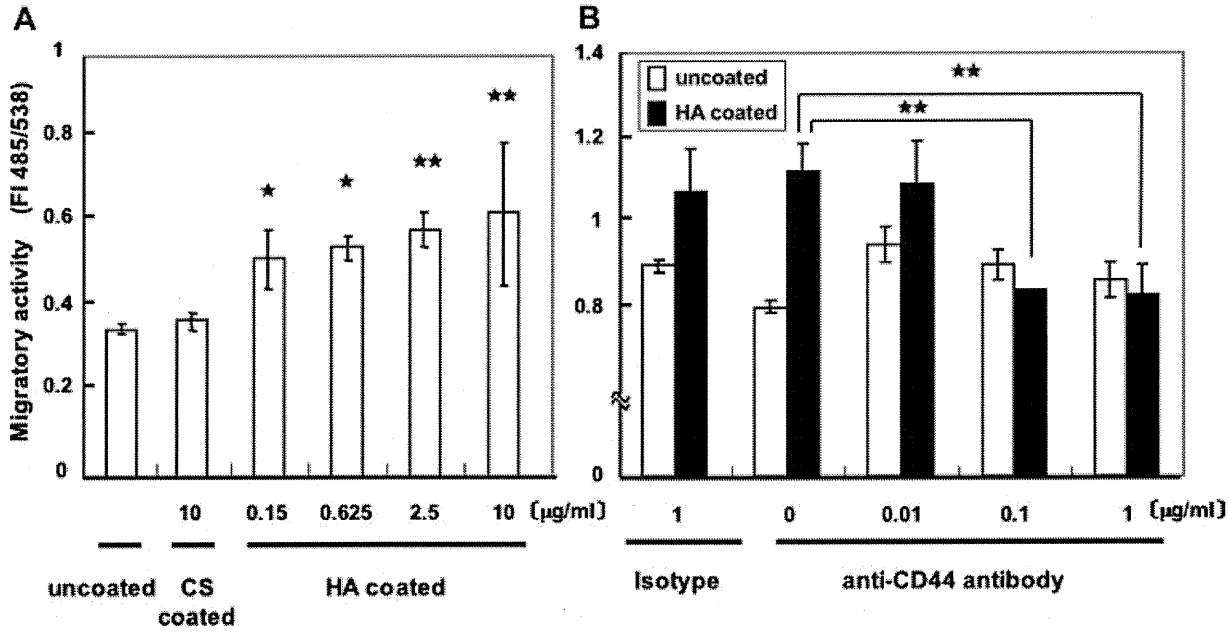

Fig. 6. HA facilitates MPDL22 migration via HA/CD44 pathway. MPDL22 cells (1×10^5 cell/well) were added to the upper chamber of an insert membrane filter which had been coated with HA (1 μg/ml) or CS (1 μg/ml) in 96-well culture plates and cultured for 24 h in the presence (B) or absence (A) of anti-CD44 antibody or isotype control antibody. Migratory cells on the bottom of the insert membrane were dissociated from the membrane with cell detachment buffer. These cells were subsequently lysed and detected by the CyQuant GR dye. The intensity of fluorescence was measured with a fluorescence plate reader. Results of one representative experiment out of three separate experiments are shown. The results are presented as mean value ± SEM (n = 3) ($^{**}P \leq 0.01$ vs. CS coated control (A), $^{**}P < 0.01$ (B)).

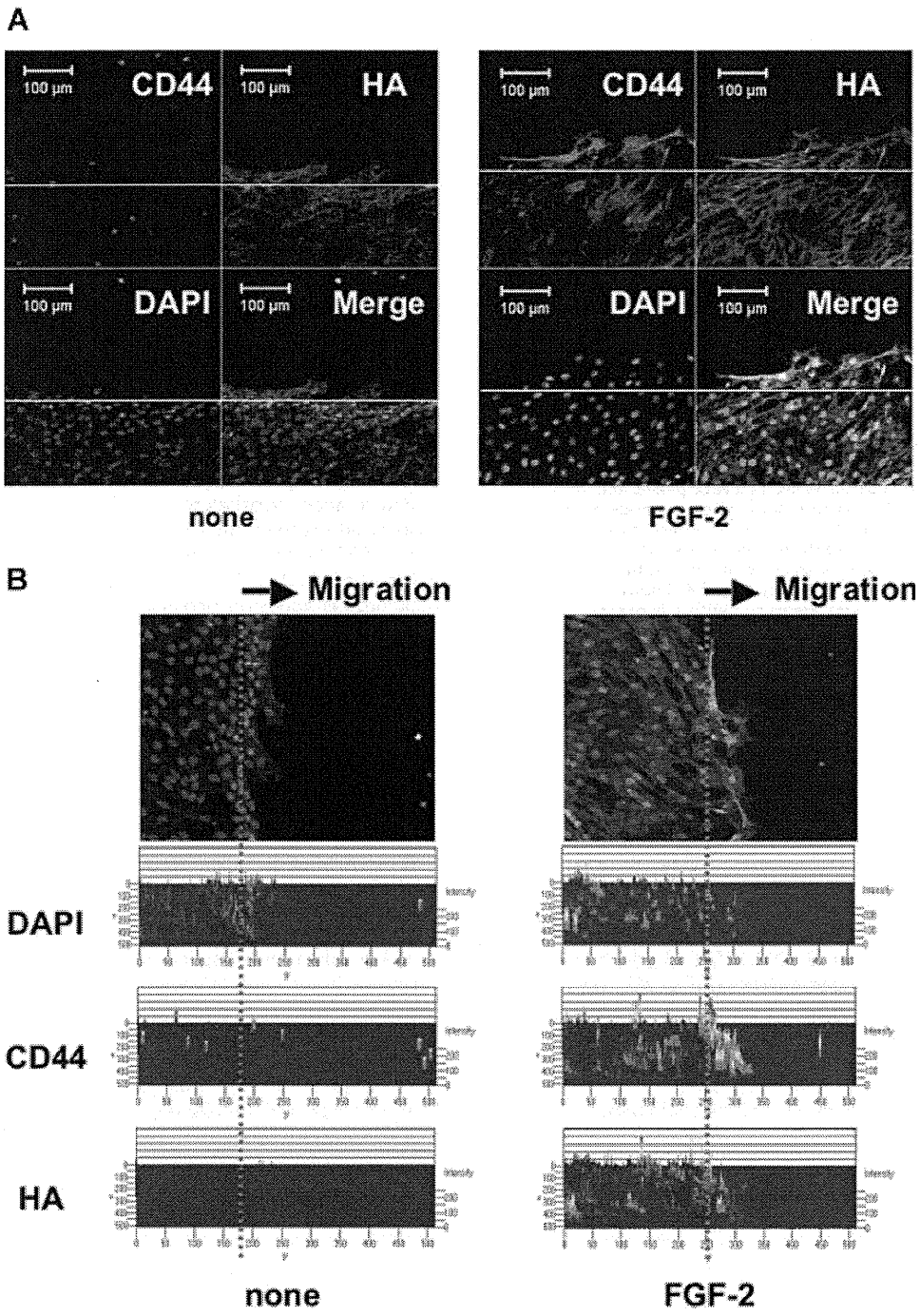

Fig. 7. FGF-2-stimulated migratory MPDL22 cells showed increased CD44 expression colocalized with HA. A: MPDL22 cells (5×10^4 cell/well) were seeded behind a silicon rubber on a coverglass mounted on a 35-mm dish and allowed to reach confluence. After carefully removing the silicon rubber, the monolayers were incubated with or without FGF-2 (5 ng/ml). Cells were fixed for 10 min with 4% paraformaldehyde. After blocking with 1% BSA, the cell monolayer was incubated with rat anti-mouse CD44 followed by washing with PBS and Alexa Fluor 546 conjugated goat anti-rat antibody for 30 min. Cells were incubated with biotinylated HA binding protein and then FITC–avidin. Cells were washed with PBS between each step. Cells were counterstained with DAPI. Dotted lines are the edge of the cell layer just after removing the silicon rubber. Results of one representative experiment out of three separate experiments are shown. B: The photographs were quantified as described in the Materials and Methods Section. Dotted lines are the edge of the cell layer just after removing the silicon rubber.

less migratory activity for the HA-coated chamber (Zhu et al., 2006). Integrins play a key role in cell motility via interactions with extracellular matrices (Juliano et al., 2004). In this study, we demonstrated that FGF-2 enhanced the migratory activity of PDL cells via the interaction with CD44 and HA.

The proliferative responses may influence the migratory activity. While the significant increase in proliferation of MPDL22 was not seen 12 h after FGF-2 stimulation (data not shown), the migratory activity was observed at that time (Fig. 1). In addition, FGF-2-dependent migratory activity of MPDL22

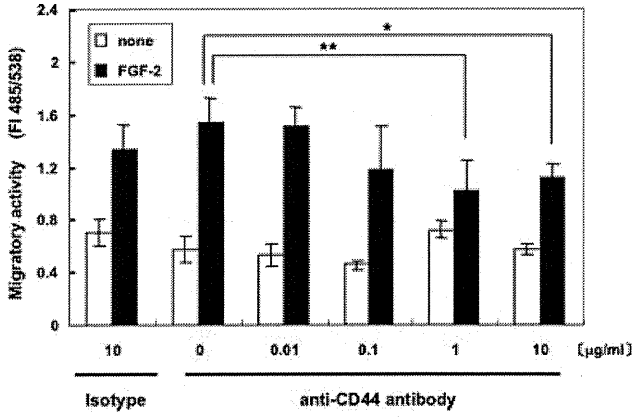

Fig. 8. CD44 mediated FGF-2-activated migration of MPDL22 cells. MPDL22 cells (1×10^5 cell/well) were added to the upper chamber of an insert membrane filter in 96-well culture plates and stimulated with or without FGF-2 (5 ng/ml). Anti-CD44 antibody or isotype control antibody was added to the well. The cells migrating to the bottom of the insert membrane were dissociated from the membrane when incubated with cell detachment buffer. These cells were subsequently lysed and detected by the CyQuant GR dye. The intensity of fluorescence was measured with a fluorescence plate reader. Results of one representative experiment out of three separate experiments are shown. The results are presented as mean value ± SEM (n = 3) ($^*P < 0.05$, $^{**}P < 0.01$).

cells remained statistically significant 24 h after stimulation with FGF-2 even when the proliferative response of MPDL22 was completely suppressed by mitomycin C treatment (Fig. 1C,D).

FGF-2 activated cell proliferation of PDL cells and ERK1/2 signaling molecule, one important pathway among downstream effectors of FGF receptors, mediates the proliferative response but PI3K does not (data not shown). Treatment of MPDL22 with 2 nM Wortmannin and 2 μM LY294002, which significantly inhibited the FGF-2-induced migration (Fig. 2C), did not affect the proliferation regardless of the presence or absence of FGF-2 stimulation (data not shown). These results suggest that FGF-2 uses distinct intracellular signaling pathways to control migration and proliferation of MPDL22.

Akt is a downstream effector of the PI3K-dependent signaling cascade and is stimulated by various kinds of growth factors including FGF-2. Previous reports demonstrated that FGF-2-induced phosphorylation of akt depends on PI3K signaling (Datta et al., 1999; Schmidt et al., 2006; Johnson-Farley et al., 2007). In addition, we found that FGF-2-stimulated akt phosphorylation in MPDL22 was completely inhibited by the PI3K inhibitors, Wortmannin and LY294002 (data not shown). These results suggest that akt is a downstream effector of PI3K and activated solely via the PI3K pathway in FGF-2-stimulated MPDL22.

Akt activates several factors such as p21-activated kinase, Src homologous, p70S6K, and EDG-1, which lead to rearrangement of the actin cytoskeleton (Han et al., 1995; King et al., 2000; Qian et al., 2004). Recently, it was demonstrated that actin was a major partner among proteins which co-immunoprecipitated with akt and that FGF-2 stimulation strongly upregulated the association between actin and akt (Vandermoere et al., 2007). Thus, by interacting with the actin cytoskeleton, akt is thought to play a key role in the subsequent migration of MPDL22 cells in response to FGF-2.

The expression of CD44 is upregulated within injured or inflammatory tissues (Foster et al., 1998; Pure and Cuff, 2001). Furthermore, CD44 has been reported to function as a regulator of the cell motility and chemotaxis (Katagiri et al., 1999). TNFα-upregulated CD44 expression is accompanied by cell migration in ovarian cancer cells (Muthukumaran et al., 2006). In this study, the level of CD44 expression was increased in migratory FGF-2-stimulated MPDL22. Thus, we speculated that CD44 plays an important role in the migration of MPDL22 cells as well as other types of cells.

Several kinds of signaling pathways are involved in cytokine-induced CD44 expression. Rho signaling is pivotal for CD44 expression (Chellaiah et al., 2003; Desai et al., 2007) and Rho kinase, Rho downstream effector, enhanced CD44 expression through CD44/ezrin/radixin/moesin (ERM)/actin complex formation (Chellaiah et al., 2003). Since bisphosphonate, whose target is Rho signaling, reduced the expression of CD44 and FGF-2-dependent cell migration (data not shown), Rho family appears to mediate the induction of CD44 and cell migration by FGF-2 in MPDL22.

CD44 functions as a receptor for extracellular matrices such as collagen, fibronectin, osteopontin, and HA. The interactions between CD44 and such extracellular matrices transduce various signaling pathways. The cytoplasmic domain of CD44 is linked to actin cytoskeleton and interacts with cytoskeletal-associated proteins such as ERM and ankyrin (Bourguignon et al., 1992; Hirao et al., 1996; Yonemura et al., 1998), resulting in cytoskeleton activation and cause several biological functions including cell adhesion, proliferation, and migration (Lokeshwar et al., 1994, 1996; Zhu and Bourguignon, 1998). Interestingly, CD44/HA interaction leads to activation of Ras signaling (Sohara et al., 2001) and PI3K pathway (Katso et al., 2001). In this study, we found that application of PI3K inhibitor to HA-coated transwell migration assay inhibited MPDL22 migration (data not shown). Thus, CD44/HA interaction may activate the migration of MPDL22 at least in part via PI3K molecules. It remains unclear whether the mechanism by which PI3K is activated in CD44/HA stimulation is different from that in FGF-2 stimulation. However, we speculated that FGF-2 induces both the immediate activation via FGFR to initiate cell migration and the delayed and the sustained stimulation by the CD44/HA interaction to prolong and maintain the migration.

HA production is implicated in cell proliferation and migration in response to growth factors or tissue injury (Tammi and Tammi, 1991; Savani et al., 1995; Evanko et al., 2001). As shown in Figure 5D, FGF-2 altered mRNA expression of not only Has-1, Has-2, and Has-3 but also Hyal-1, Hyal-2, Hyal-3. However, FGF-2 did not alter the molecular mass of HA produced by MPDL22 (Fig. 5C). These results suggest that FGF-2-stimulated migration of MPDL22 was at least partially dependent on the increased HA production but not the change in the molecular mass of the HA. In this study, FACS and immunocytochemical analyses revealed that FGF-2 enhanced the expression of both CD44 and HA and the binding avidity between these molecules. In addition, the CD44 expression on FGF-2-activated migrating MPDL22 cells was co-localized with HA (Fig. 7). These findings suggest that FGF-2 activates MPDL22 to migrate through CD44/HA engagement with upregulation of CD44 binding activity and HA expression.

Several cell surface receptors including RHAMM, LYVE-1, Layilin are also known to bind to HA. HA-induced regulation of cell function via HA receptors vary depending on the differences in cell type, cell origin, HA size. In this study, the involvement of other HA receptors in HA-mediated migration of MPDL22 cells was not investigated. However, the fact that the anti-CD44 antibody completely abolished the HA-induced cell migration (Fig. 6B) suggests that CD44 is mainly involved in the HA-dependent migration of MPDL22 cells. Furthermore, the fact that anti-CD44 antibody did not completely inhibit the FGF-2-induced cell migration (Fig. 8) suggested that not only HA–CD44 but also other interactions should be involved in the migration.

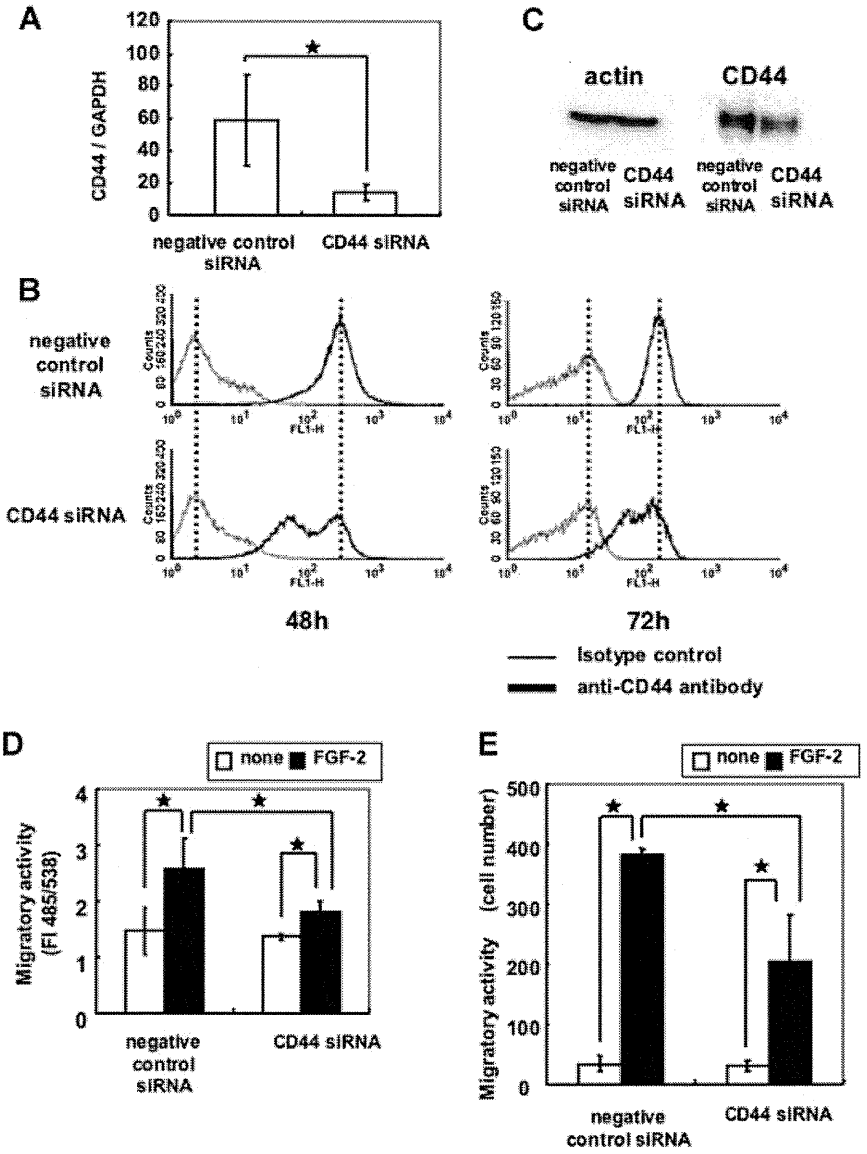

Fig. 9. Silencing CD44 by siRNA suppressed the migration of MPDL22. A: MPDL22 cells transfected with CD44 siRNA or negative control siRNA were cultured for 24 h. CD44 mRNA was quantified by real-time PCR. Results of one representative experiment out of three separate experiments are shown. The results are presented as mean value ± SEM (n = 3) (*$P < 0.05$). B: MPDL22 cells transfected with CD44 siRNA or negative control siRNA were cultured for 48 or 72 h. The cells were incubated with rat anti-mouse CD44 and then washed with PBS and treated with FITC-labeled-goat polyclonal anti-rat IgG. Cells were analyzed by flow cytometry. Results of one representative experiment out of three separate experiments are shown. C: MPDL22 transfected with CD44 siRNA or negative control siRNA were cultured for 48 h. The cells were lyzed and the proteins were electrophoresed on 8% mini-gels, transblotted onto nitrocellulose membrane and immunoreactive CD44 was detected using a primary anti-CD44 antibody, anti-actin antibody, HRP-conjugated secondary antibody, and chemiluminescence kit. As a control, actin was detected using anti-actin antibody. Results of one representative experiment out of three separate experiments are shown. D: MPDL22 cells (5×10^4 cell/well) were transfected with CD44 siRNA or negative control siRNA were added to the upper chamber of an insert membrane filter of with a pore size of 8 μm in 96-well culture plates and stimulated with or without FGF-2 (5 ng/ml) for 12 h. Cells migrating to the bottom of the insert membrane were dissociated from the membrane with cell detachment buffer. These cells were subsequently lysed and detected by the CyQuant GR dye. The intensity of fluorescence was measured with a fluorescence plate reader. Results of one representative experiment out of three separate experiments are shown. The results are presented as mean value ± SEM (n = 3) (*$P < 0.05$). E: MPDL22 cells (5×10^4 cell/well) were transfected with CD44 siRNA or negative control siRNA were seeded behind a silicon rubber on a coverglass mounted on a 35-mm dish and allowed to reach confluence. After carefully removing the silicon rubber, the monolayers were incubated with or without FGF-2 (5 ng/ml) for 12 h. Then the cells were fixed in 4% paraformaldehyde for 10 min. The number of cells migrating into the cell-free area was counted as described in the Materials and Methods Section. Results of one representative experiment out of three separate experiments are shown. The results are presented as mean values ± SEM (n = 3) (*$P < 0.05$).

Perimembranous osteopontin which was co-localized with CD44 at the leading edge in migratory fibroblasts that appears to participate in cell migration, probably associated with the cytoplasmic portion of CD44 (Zohar et al., 2000). We also found that FGF-2 induced the expression of the intracellular osteopontin in migratory MPDL22 (data not shown). This suggests that FGF-2 regulates not only the production but also the localization of ECM and in turn enhances the cell migration.

The present study demonstrated that FGF-2 induces the migration of MPDL22 cells via PI3K/akt and CD44/HA pathways.

The orchestrated action of FGF-2 described above seems to play a key role in stimulating regeneration of periodontal tissue. Recently, topical application of FGF-2 was reported to be efficacious in regenerating periodontal tissues of periodontitis patients (Kitamura et al., 2008, 2010). In addition, our previous in vitro studies showed that FGF-2 facilitates cell proliferation and the production of various types of extracellular matrix (Takayama et al., 1997; Shimabukuro et al., 2005; Terashima et al., 2008). This suggests that FGF-2 not only stimulates the proliferation of PDL cells but also provides a favorable local environment for cell migration, which facilitates periodontal tissue regeneration.

Acknowledgments

This study was supported by the Japan Society for the Promotion of Science (20390529, 20390530, 20592427 21592623, 21659482, 21890137, and 22592182) and Research Fellow of the Japan Society for the Promotion of Science.

Literature Cited

Acharya PS, Majumdar S, Jacob M, Hayden J, Mrass P, Weninger W, Assoian RK, Pure E. 2008. Fibroblast migration is mediated by CD44-dependent TGF beta activation. J Cell Sci 121:1393–1402.

Beertsen W, McCulloch CA, Sodek J. 1997. The periodontal ligament: A unique, multifunctional connective tissue. Periodontology 2000 13:20–40.

Bourguignon LY, Gilad E, Peyrollier K, Brightman A, Swanson RA. 2007. Hyaluronan-CD44 interaction stimulates Rac1 signaling and PKN gamma kinase activation leading to cytoskeleton function and cell migration in astrocytes. J Neurochem 101:1002–1017.

Bourguignon LY, Lokeshwar VB, He J, Chen X, Bourguignon GJ. 1992. A CD44-like endothelial cell transmembrane glycoprotein (GP116) interacts with extracellular matrix and ankyrin. Mol Cell Biol 12:4464–4471.

Bourguignon LY, Zhu H, Shao L, Chen YW. 2000. CD44 interaction with tiam1 promotes Rac1 signaling and hyaluronic acid-mediated breast tumor cell migration. J Biol Chem 275:1829–1838.

Cantley LC. 2002. The phosphoinositide 3-kinase pathway. Science 296:1655–1657.

Chellaiah MA, Biswas RS, Rittling SR, Denhardt DT, Hruska KA. 2003. Rho-dependent Rho kinase activation increases CD44 surface expression and bone resorption in osteoclasts. J Biol Chem 278:29086–29097.

Datta SR, Brunet A, Greenberg ME. 1999. Cellular survival: A play in three Akts. Genes Dev 13:2905–2927.

Derman MP, Toker A, Hartwig JH, Spokes K, Falck JR, Chen CS, Cantley LC, Cantley LG. 1997. The lipid products of phosphoinositide 3-kinase increase cell motility through protein kinase C. J Biol Chem 272:6465–6470.

Desai B, Rogers MJ, Chellaiah MA. 2007. Mechanisms of osteopontin and CD44 as metastatic principles in prostate cancer cells. Mol Cancer 6:18.

Evanko SP, Johnson PY, Braun KR, Underhill CB, Dudhia J, Wight TN. 2001. Platelet-derived growth factor stimulates the formation of versican-hyaluronan aggregates and pericellular matrix expansion in arterial smooth muscle cells. Arch Biochem Biophys 394:29–38.

Fanning A, Volkov Y, Freeley M, Kelleher D, Long A. 2005. CD44 cross-linking induces protein kinase C-regulated migration of human T lymphocytes. Int Immunol 17:449–458.

Foster LC, Arkonac BM, Sibinga NE, Shi C, Perrella MA, Haber E. 1998. Regulation of CD44 gene expression by the proinflammatory cytokine interleukin-1beta in vascular smooth muscle cells. J Biol Chem 273:20341–20346.

Goodison S, Urquidi V, Tarin D. 1999. CD44 cell adhesion molecules. Mol Pathol 52:189–196.

Han JW, Pearson RB, Dennis PB, Thomas G. 1995. Rapamycin, wortmannin, and the methylxanthine SQ20006 inactivate p70s6k by inducing dephosphorylation of the same subset of sites. J Biol Chem 270:21396–21403.

Hirao M, Sato N, Kondo T, Yonemura S, Monden M, Sasaki T, Takai Y, Tsukita S. 1996. Regulation mechanism of ERM (ezrin/radixin/moesin) protein/plasma membrane association: Possible involvement of phosphatidylinositol turnover and Rho-dependent signaling pathway. J Cell Biol 135:37–51.

Johnson-Farley NN, Patel K, Kim D, Cowen DS. 2007. Interaction of FGF-2 with IGF-1 and BDNF in stimulating Akt, ERK, and neuronal survival in hippocampal cultures. Brain Res 1154:40–49.

Jones LL, Liu Z, Shen J, Werner A, Kreutzberg GW, Raivich G. 2000. Regulation of the cell adhesion molecule CD44 after nerve transection and direct trauma to the mouse brain. J Comp Neurol 426:468–492.

Juliano RL, Reddig P, Alahari S, Edin M, Howe A, Aplin A. 2004. Integrin regulation of cell signalling and motility. Biochem Soc Trans 32:443–446.

Katagiri YU, Sleeman J, Fujii H, Herrlich P, Hotta H, Tanaka K, Chikuma S, Yagita H, Okumura K, Murakami M, Saiki I, Chambers AF, Uede T. 1999. CD44 variants but not CD44s cooperate with beta1-containing integrins to permit cells to bind to osteopontin independently of arginine-glycine-aspartic acid, thereby stimulating cell motility and chemotaxis. Cancer Res 59:219–226.

Katso R, Okkenhaug K, Ahmadi K, White S, Timms J, Waterfield MD. 2001. Cellular function of phosphoinositide 3-kinases: Implications for development, homeostasis, and cancer. Annu Rev Cell Dev Biol 17:615–675.

King TR, Fang Y, Mahon ES, Anderson DH. 2000. Using a phage display library to identify basic residues in A-Raf required to mediate binding to the Src homology 2 domains of the p85 subunit of phosphatidylinositol 3′-kinase. J Biol Chem 275:36450–36456.

Kitamura M, Nakashima K, Kowashi Y, Fujii T, Shimauchi H, Sasano T, Furuuchi T, Fukuda M, Noguchi T, Shibutani T, Iwayama Y, Takashiba S, Kurihara H, Ninomiya M, Kido J, Nagata T, Hamachi T, Maeda K, Hara Y, Izumi Y, Hirofuji T, Imai E, Omae M, Watanuki M, Murakami S. 2008. Periodontal tissue regeneration using fibroblast growth factor-2: Randomized controlled phase II clinical trial. PLoS ONE 3:e2611.

Kitamura M, Akamatsu M, Machigashira M, Hara Y, Sakagami R, Hirofuji T, Hamachi T, Maeda K, Yokota M, Kido J, Nagata T, Kurihara H, Takashiba S, Shibutani T, Fukuda M, Noguchi T, Yamazaki K, Yoshie H, Ioroi K, Arai T, Nakagawa T, Ito K, Oda S, Izumi Y, Ogata Y, Yamada S, Shimauchi H, Kunimatsu K, Kawanami M, Fujii T, Furuichi Y, Furuuchi T, Sasano T, Imai E, Omae M, Yamada S, Watanuki M, Murakami S. 2010. FGF-2 stimulates periodontal regeneration: Results of a multi-center randomized clinical trial. J Dent Res (in press).

Lammi PE, Lammi MJ, Tammi RH, Helminen HJ, Espanha MM. 2001. Strong hyaluronan expression in the full-thickness rat articular cartilage repair tissue. Histochem Cell Biol 115:301–308.

Lee HG, Cowman MK. 1994. An agarose gel electrophoretic method for analysis of hyaluronan molecular weight distribution. Anal Biochem 219:278–287.

Legg JW, Lewis CA, Parsons M, Ng T, Isacke CM. 2002. A novel PKC-regulated mechanism controls CD44 ezrin association and directional cell motility. Nat Cell Biol 4:399–407.

Lekic PC, Rajshankar D, Chen H, Tenenbaum H, McCulloch CA. 2001. Transplantation of labeled periodontal ligament cells promotes regeneration of alveolar bone. Anat Rec 262:193–202.

Lokeshwar VB, Fregien N, Bourguignon LY. 1994. Ankyrin-binding domain of CD44(GP85) is required for the expression of hyaluronic acid-mediated adhesion function. J Cell Biol 126:1099–1109.

Lokeshwar VB, Iida N, Bourguignon LY. 1996. The cell adhesion molecule, GP116, is a new CD44 variant (ex14/v10) involved in hyaluronic acid binding and endothelial cell proliferation. J Biol Chem 271:23853–23864.

Maheshwari G, Wiley HS, Lauffenburger DA. 2001. Autocrine epidermal growth factor signaling stimulates directionally persistent mammary epithelial cell migration. J Cell Biol 24:1123–1128.

Murakami S, Takayama S, Ikezawa K, Shimabukuro Y, Kitamura M, Nozaki T, Terashima A, Asano T, Okada H. 1999. Regeneration of periodontal tissues by basic fibroblast growth factor. J Periodontal Res 34:425–430.

Murakami S, Takayama S, Kitamura M, Shimabukuro Y, Yanagi K, Ikezawa K, Saho T, Nozaki T, Okada H. 2003. Recombinant human basic fibroblast growth factor (bFGF) stimulates periodontal regeneration in class II furcation defects created in beagle dogs. J Periodontal Res 38:97–103.

Murakami S. 2010. Periodontal tissue regeneration by signalling molecule(s)—Does FGF-2innovate on the periodontal therapy? Periodontology 2000 (in press).

Muthukumaran N, Miletti-Gonzalez KE, Ravindranath AK, Rodriguez-Rodriguez L. 2006. Tumor necrosis factor-alpha differentially modulates CD44 expression in ovarian cancer cells. Mol Cancer Res 4:511–520.

Mylona E, Jones KA, Mills ST, Pavlath GK. 2006. CD44 regulates myoblast migration and differentiation. J Cell Physiol 209:314–321.

Pure E, Cuff CA. 2001. A crucial role for CD44 in inflammation. Trends Mol Med 7:213–221.

Qian Y, Corum L, Meng Q, Blenis J, Zheng JZ, Shi X, Flynn DC, Jiang BH. 2004. PI3K induced actin filament remodeling through Akt and p70S6K1: Implication of essential role in cell migration. Am J Physiol Cell Physiol 286:C153–C163.

Raja RH, LeBoeuf RD, Stone GW, Weigel PH. 1984. Preparation of alkylamine and 125I-radiolabeled derivatives of hyaluronic acid uniquely modified at the reducing end. Anal Biochem 139:168–177.

Ren XD, Schwartz MA. 1998. Regulation of inositol lipid kinases by Rho and Rac. Curr Opin Genet Dev 8:63–67.

Savani RC, Wang C, Yang B, Zhang S, Kinsella MG, Wight TN, Stern R, Nance DM, Turley EA. 1995. Migration of bovine aortic smooth muscle cells after wounding injury. The role of hyaluronan and RHAMM. J Clin Invest 95:1158–1168.

Schmidt A, Ladage D, Schinkothe T, Klausmann U, Ulrichs C, Klinz FJ, Brixius K, Arnhold S, Desai B, Mehlhorn U, Schwinger RH, Staib P, Addicks K, Bloch W. 2006. Basic fibroblast growth factor controls migration in human mesenchymal stem cells. Stem Cells 24:1750–1758.

Seo BM, Miura M, Gronthos S, Bartold PM, Batouli S, Brahim J, Young M, Robey PG, Wang CY, Shi S. 2004. Investigation of multipotent postnatal stem cells from human periodontal ligament. Lancet 364:149–155.

Shimabukuro Y, Ichikawa T, Takayama S, Yamada S, Takedachi M, Terakura M, Hashikawa T, Murakami S. 2005. Fibroblast growth factor-2 regulates the synthesis of hyaluronan by human periodontal ligament cells. J Cell Physiol 203:557–563.

Smith JT, Tomfohr JK, Wells MC, Beebe TP, Jr., Kepler TB, Reichert WM. 2004. Measurement of cell migration on surface-bound fibronectin gradients. Langmuir 20:8279–8286.

Sohara Y, Ishiguro N, Machida K, Kurata H, Thant AA, Senga T, Matsuda S, Kimata K, Iwata H, Hamaguchi M. 2001. Hyaluronan activates cell motility of v-Src-transformed cells via Ras-mitogen-activated protein kinase and phosphoinositide 3-kinase-Akt in a tumor-specific manner. Mol Biol Cell 12:1859–1868.

Takayama S, Murakami S, Miki Y, Ikezawa K, Tasaka S, Terashima A, Asano T, Okada H. 1997. Effects of basic fibroblast growth factor on human periodontal ligament cells. J Periodontal Res 32:667–675.

Takayama S, Murakami S, Shimabukuro Y, Kitamura M, Okada H. 2001. Periodontal regeneration by FGF-2 (bFGF) in primate models. J Dent Res 80:2075–2079.

Tammi R, Tammi M. 1991. Correlations between hyaluronan and epidermal proliferation as studied by [3H]glucosamine and [3H]thymidine incorporations and staining of hyaluronan on mitotic keratinocytes. Exp Cell Res 195:524–527.

Terashima Y, Shimabukuro Y, Terashima H, Ozasa M, Terakura M, Ikezawa K, Hashikawa T, Takedachi M, Oohara H, Yamada S, Murakami S. 2008. Fibroblast growth factor-2 regulates expression of osteopontin in periodontal ligament cells. J Cell Physiol 216:640–650.

Thorne RF, Legg JW, Isacke CM. 2004. The role of the CD44 transmembrane and cytoplasmic domains in co-ordinating adhesive and signalling events. J Cell Sci 117:373–380.

Vandermoere F, El Yazidi-Belkoura I, Demont Y, Slomianny C, Antol J, Lemoine J, Hondermarck H. 2007. Proteomics exploration reveals that actin is a signaling target of the kinase Akt. Mol Cell Proteomics 6:114–124.

Weiner OD, Neilsen PO, Prestwich GD, Kirschner MW, Cantley LC, Bourne HR. 2002. A PtdInsP(3)- and Rho GTPase-mediated positive feedback loop regulates neutrophil polarity. Nat Cell Biol 4:509–513.

Yamada S, Tomoeda M, Ozawa Y, Yoneda S, Terashima Y, Ikezawa K, Ikegawa S, Saito M, Toyosawa S, Murakami S. 2007. PLAP-1/asporin, a novel negative regulator of periodontal ligament mineralization. J Biol Chem 282:23070–23080.

Yonemura S, Hirao M, Doi Y, Takahashi N, Kondo T, Tsukita S. 1998. Ezrin/radixin/moesin (ERM) proteins bind to a positively charged amino acid cluster in the juxta-membrane cytoplasmic domain of CD44, CD43, and ICAM-2. J Cell Biol 140:885–895.

Zhu D, Bourguignon LY. 1998. The ankyrin-binding domain of CD44s is involved in regulating hyaluronic acid-mediated functions and prostate tumor cell transformation. Cell Motil Cytoskeleton 39:209–222.

Zhu H, Mitsuhashi N, Klein A, Barsky LW, Weinberg K, Barr ML, Demetriou A, Wu GD. 2006. The role of the hyaluronan receptor CD44 in mesenchymal stem cell migration in the extracellular matrix. Stem Cells 24:928–935.

Zohar R, Suzuki N, Suzuki K, Arora P, Glogauer M, McCulloch CA, Sodek J. 2000. Intracellular osteopontin is an integral component of the CD44-ERM complex involved in cell migration. J Cell Physiol 184:118–130.

Biochemical and Biophysical Research Communications 403 (2010) 345–350

Contents lists available at ScienceDirect

Biochemical and Biophysical Research Communications

journal homepage: www.elsevier.com/locate/ybbrc

Effects of concomitant use of fibroblast growth factor (FGF)-2 with beta-tricalcium phosphate (β-TCP) on the beagle dog 1-wall periodontal defect model

Jun Anzai [a,b], Masahiro Kitamura [b], Takenori Nozaki [b], Toshie Nagayasu [a], Akio Terashima [a], Taiji Asano [a], Shinya Murakami [b,*]

[a] Pharmacology Department, Central Research Laboratories, Kaken Pharmaceutical Co., Ltd., 14, Shinomiya, Minamigawara-cho, Yamashina-ku, Kyoto 607-8042, Japan
[b] Department of Periodontology, Osaka University Graduate School of Dentistry, 1-8 Yamadaoka, Suita, Osaka 565-0871, Japan

ARTICLE INFO

Article history:
Received 25 October 2010
Available online 13 November 2010

Keywords:
FGF-2
Periodontal regeneration
Cytokine therapy
β-TCP
Beagle dog

ABSTRACT

The effects of concomitant use of fibroblast growth factor-2 (FGF-2) and beta-tricalcium phosphate (β-TCP) on periodontal regeneration were investigated in the beagle dog 1-wall periodontal defect model. One-wall periodontal defects were created in the mesial portion of both sides of the mandibular first molars, and 0.3% FGF-2 plus β-TCP or β-TCP alone was administered. Radiographic evaluation was performed at 0, 3, and 6 weeks. At 6 weeks, the periodontium with the defect site was removed and histologically analyzed.

Radiographic findings showed that co-administration of FGF-2 significantly increased bone mineral contents of the defect sites compared with β-TCP alone. Histologic analysis revealed that the length of the regenerated periodontal ligament, the cementum, distance to the junctional epithelium, new bone height, and area of newly formed bone were significantly increased in the FGF-2 group. No abnormal inflammatory response or ankylosis was observed in either group. These findings indicate the efficacy of concomitant use of FGF-2 and β-TCP as an osteoconductive material for periodontal regeneration following severe destruction by progressive periodontitis.

1. Introduction

Periodontitis is an inflammatory disease caused by periodontopathic bacteria. As periodontitis worsens, the alveolar bone supporting the teeth is absorbed and teeth are eventually lost. Conventional treatment for periodontitis involves the mechanical removal of bacterial biofilms (dental plaque) and dental calculus including periodontopathic microorganisms, via scaling and root planning. In severe cases, in which resorption of alveolar bone has progressed, periodontal surgery is needed. However, no conventional periodontal and/or surgical treatments can regenerate lost periodontal tissue or its functionality. To deal with this dental limitation, guided tissue regeneration (GTR) [1], which induces periodontal regeneration by keeping gingiva out of the defect and reserving space for new bone, the periodontal ligament, and the cementum, was developed in the early 1980s and has been clinically adopted.

Alternative methods that enhance periodontal regeneration by activating the proliferation of mesenchymal progenitor cells in the periodontal ligament and differentiation to hard tissue-forming cells by local administration of signaling molecules have also been investigated. Studies directed at clinical use have progressed, including use of enamel matrix derivative (EMD) [2], platelet-derived growth factor-BB (PDGF-BB) [3], concomitant use of PDGF-BB and insulin-like growth factor-1 [4,5], bone morphogenic protein (BMP)-2 [6–9], transforming growth factor-β (TGF-β) [10], BMP-7 [11], brain-derived neurotrophic factor (BDNF) [12], and growth and differentiation factor-5 (GDF-5) [13]. The combination of 0.03% PDGF-BB plus granular β-tricalcium phosphate (β-TCP) was approved by the US Food and Drug Administration FDA in 2005 and is available as a medical device for periodontal regeneration in the United States.

We have intensively investigated the induction of periodontal regeneration with fibroblast growth factor-2 (FGF-2) [14,15]. We demonstrated that FGF-2 enhanced the regeneration of alveolar bone, the cementum, and the periodontal ligament in beagle dog 2-wall, 3-wall [16], and class II furcation defects [17] as well as non-human primate class II furcation defect models [18]. Based on these results, we conducted a phase II clinical trial of 2-wall and 3-wall defects in patients with periodontitis, confirmed the

* Corresponding author. Fax: +81 6 6879 2934.
E-mail addresses: anzai_jun@kaken.co.jp (J. Anzai), kitamura@dent.osaka-u.ac.jp (M. Kitamura), tnozaki@dent.osaka-u.ac.jp (T. Nozaki), nagayasu_toshie@kaken.co.jp (T. Nagayasu), terashima_akio@kaken.co.jp (A. Terashima), asano_taiji@kaken.co.jp (T. Asano), ipshinya@dent.osaka-u.ac.jp (S. Murakami).

0006-291X/$ - see front matter © 2010 Elsevier Inc. All rights reserved.
doi:10.1016/j.bbrc.2010.11.032